IGNITION DELAY TIMES OF NATURAL GAS/HYDROGEN BLENDS AT ELEVATED PRESSURES

A Thesis

by

MARISSA LYNN BROWER

Submitted to the Office of Graduate Studies of
Texas A&M University
in partial fulfillment of the requirements for the degree of

MASTER OF SCIENCE

August 2012

Major Subject: Mechanical Engineering

Ignition Delay Times of Natural Gas/Hydrogen Blends at Elevated Pressures

IGNITION DELAY TIMES OF NATURAL GAS/HYDROGEN BLENDS AT ELEVATED PRESSURES

A Thesis

by

MARISSA LYNN BROWER

Submitted to the Office of Graduate Studies of
Texas A&M University
in partial fulfillment of the requirements for the degree of

MASTER OF SCIENCE

Approved by:

Chair of Committee,	Eric Petersen
Committee Members,	Rodney Bowersox
	Felix Güthe
	David Staack
Head of Department,	Jerald Caton

August 2012

Major Subject: Mechanical Engineering

ABSTRACT

Ignition Delay Times of Natural Gas/Hydrogen Blends

at Elevated Pressures. (August 2012)

Marissa Lynn Brower, B.S., Rice University

Chair of Advisory Committee: Dr. Eric L. Petersen

Applications of natural gases that contain high levels of hydrogen have become a primary interest in the gas turbine market. For reheat gas turbines, understanding of the ignition delay times of high-hydrogen natural gases is important for two reasons. First, if the ignition delay time is too short, autoignition can occur in the mixer before the primary combustor. Second, the flame in the secondary burner is stabilized by the ignition delay time of the fuel. While the ignition delay times of hydrogen and of the individual hydrocarbons in natural gases can be considered well known, there have been few previous experimental studies into the effects of different levels of hydrogen on the ignition delay times of natural gases at gas turbine conditions.

In order to examine the effects of hydrogen content at gas turbine conditions, shock-tube experiments were performed on nine combinations of an L9 matrix. The L9 matrix was developed by varying four factors: natural gas higher-order hydrocarbon content of 0, 18.75, or 37.5%; hydrogen content of the total fuel mixture of 30, 60, or 80%; equivalence ratios of 0.3, 0.5, or 1; and pressures of 1, 10, or 30 atm. Temperatures ranged from 1092 K to 1722 K, and all mixtures were diluted in 90% Ar. Correlations

for each combination were developed from the ignition delay times and, using these correlations, a factor sensitivity analysis was performed. It was found that hydrogen played the most significant role in ignition delay time. Pressure was almost as important as hydrogen content, especially as temperature increased. Equivalence ratio was slightly more important than hydrocarbon content of the natural gas, but both were less important than pressure or hydrogen content.

Further analysis was performed using ignition delay time calculations for the full matrix of combinations (27 combinations for each natural gas) using a detailed chemical kinetics mechanism. Using these calculations, separate L9 matrices were developed for each natural gas. Correlations from the full matrix and the L9 matrix for each natural gas were found to be almost identical in each case, verifying that a thoughtfully prepared L9 matrix can indeed capture the major effects of an extended matrix.

DEDICATION

I would like to dedicate this thesis to three people: my fiancé and my parents. My fiancé, Matthew Davis, has been with me for the last five years and I will be forever grateful for his constant support and for listening to my complaints. My parents, Mike and Carolyn Brower, have encouraged me throughout both my degrees and I know that I would not be the person I am today without their guidance and help.

ACKNOWLEDGMENTS

I would first like to thank my advisor and Committee Chair, Dr. Eric Petersen, for his guidance and understanding over the last two years. He has provided opportunities and experiences that have helped me academically as well as personally. I would like to thank Dr. Felix Güthe for his guidance during my internship at Alstom in Switzerland and for serving as a committee member. I would also like to thank Dr. Bowersox and Dr. Staack for serving as committee members.

Finally, I would like to thank all of my coworkers throughout the last two years. Without their support, this work would not have been possible. Specifically, I would like to thank Dr. Olivier Mathieu, Madeleine Kopp, and C. J. Aul for their help on the shock tube.

NOMENCLATURE

Variables

τ_{ign}	Ignition delay time
A	Ignition delay time correlation constant
E	Activation energy (kcal/mol-cm^3)
R	Ideal gas constant
v, w, x, y, z	Ignition delay time correlation exponents
R^2	Coefficient of multiple determination for correlations
$[i]$	Concentration of species i (mol/cm^3)
x_i	Mole fraction of species i (mol/cm^3)
P	Pressure (atm)
T	Temperature (K)
ϕ	Equivalence ratio

Abbreviations

C_{2+}	Hydrocarbons with more than 2 carbon atoms
NG	Natural Gas
HC	Hydrocarbon
NG2	Synthetic natural gas 2, described in Table 1
NG3	Synthetic natural gas 3, described in Table 1

TABLE OF CONTENTS

Page

LIST OF FIGURES

Page

LIST OF TABLES

Page

CHAPTER I

INTRODUCTION

As fuel availability changes, the need for gas turbines with greater fuel flexibility increases. Gas turbine manufacturers would like to determine if current gas turbines are flexible enough to be operated with different, sometimes lower quality, fuels while maintaining safety and mandated pollutant levels. Specifically, natural gases with high levels of hydrogen have recently become of great interest. Gaseous fuels with high levels of hydrogen can come from gasification processes like gasification of coal or biomass. However, introducing a fuel with the possibility of significantly different reactivity from traditional natural gas can lead to issues within the combustor including flashback, blowout, and changes in autoignition of the fuel. Ignition delay times of these mixtures are of primary importance because using a fuel with a significantly different ignition delay time than what is normally used in the engine could lead to ignition of the fuel in the mixer before the primary combustor, or loss of flame stability in the secondary combustor.

There is an extensive database of knowledge for the ignition delay time of methane, the primary component of natural gas, at different conditions, as well as for the primary higher-order hydrocarbons found in natural gas including ethane, propane, butane, and pentane (albeit the quantity of data varies somewhat inversely with the size of the

---

This thesis follows the style of *Combustion Science and Technology.*

hydrocarbon). Research has also fully characterized the ignition delay time chemistry of hydrogen due to the important role of the $H_2 - O_2$ system in hydrocarbon combustion and due to the importance of hydrogen as a fuel in its own right. However, there currently exist few extensive experimental studies of the ignition delay times of high levels of hydrogen mixed with different natural gases at gas turbine conditions. A recent study by Zhang et al. (2012) examined the reactivity of different levels of hydrogen addition to pure methane at elevated pressures for a constant equivalence ratio. The widely known nonlinear changes in hydrogen reactivity with temperature and pressure were seen to begin affecting the reactivity of the mixtures after the hydrogen content was greater than 60%. However, the effects of adding higher-order hydrocarbons and different equivalence ratios were not examined.

While the effects of equivalence ratio and the addition of higher-order hydrocarbons to methane are known to change the reactivity of the mixture almost linearly with temperature and pressure, it is hard to predict the reactivity of mixtures containing different levels of hydrogen without an extensive experimental approach. To reduce the number of experiments performed and still obtain meaningful results, an L9 matrix was developed. An L9 matrix is an orthogonal array that varies four different factors of the mixture, with three different levels for each factor. For this study, the four factors that were studied were base natural gas composition, hydrogen addition to the natural gas, equivalence ratio, and pressure. Using this matrix, a factor sensitivity was performed to

show the relative effects of each of the four factors. The details of this approach and the results of the study form the basis of the present thesis.

This thesis is organized into separate chapters. Chapter II provides further background on relevant gas turbine technology as well as the current knowledge of ignition delay times for the mixture components and conditions of this study. Chapter III details the L9 matrix and the experimental apparatus used for all experiments. The experimental results are shown in Chapter IV and compared to a highly validated chemical kinetics mechanism. Further discussion of the results is provided in Chapter V, including correlations developed from the experimental data and a factor sensitivity analysis. Additionally, calculations for all possible combinations for the conditions of the study were performed, and correlations are presented to show the effect of using a reduced L9 matrix for each natural gas. Finally, in Chapter VI, a brief conclusion and recommendations for further experiments are provided.

CHAPTER II

BACKGROUND

2.1 Gas Turbines

One of the largest markets for natural gas is the power generation gas turbine industry. In recent years, improvements in technology have led to the development of sequential combustion gas turbines based on the Brayton reheat cycle (Güthe et al., 2009). In Figure 1, the Brayton cycle for conventional combustion is shown next to the Brayton reheat cycle for sequential combustion. Gas turbines that employ sequential combustion first heat compressed air in the primary combustor and then send the air through a high-pressure turbine. Work is extracted from this first turbine process and then additional fuel is mixed with the air in the second combustion chamber. Combustion is again employed to raise the temperature of the gases. The gases are then sent through a low-pressure turbine and expanded a second time to extract additional work.

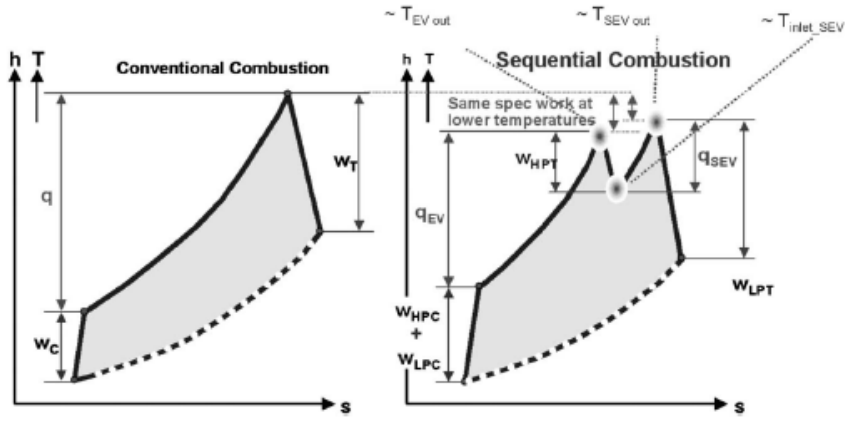

Figure 1 Brayton cycle for conventional combustion and the Brayton reheat cycle for sequential combustion. From Güthe et al. (2009).

Alstom has developed two similar sequential combustion gas turbines, the GT24 and GT26, in order to utilize the reheat concept to provide greater fuel flexibility, higher efficiency, and lower emissions (Güthe et al., 2009). Both of these turbines incorporate a primary annular combustor for the first combustion stage and a secondary, sequential burner for the second combustion stage.

Reactivity of the fuel used in a combustor of a gas turbine can play a large role in the performance, durability, and emissions of the turbine (Lieuwen et al., 2008). For a reheat gas turbine, the effects of reactivity changes have to be considered for both the primary burner and the secondary burner. In the primary burner, the main concerns are flash back and blowout. Both of these problems occur due to the changes in the laminar flame speed, causing the flame to move either too far upstream or to extinguish itself. Additionally, the ignition delay time of the fuel has to be longer than the residence time of the fuel in the mixer before the primary combustor to avoid autoignition of the fuel in the mixer.

For the secondary burner, flame stabilization is based on the ignition delay time of the fuel because higher inlet temperatures decrease the ignition delay time of the fuel (Güthe et al. 2009). The inlet temperature of the secondary burner is determined by the exit conditions of the high-pressure turbine, which is in effect controlled by the flame temperature in the primary burner. This dependence on flame temperature causes the

secondary burner inlet temperature to be almost a factor of two higher than the inlet temperature of the primary burner.

In industrial gas turbines, the combustion process often occurs at very high pressures and temperatures. Conditions in the combustors vary depending on the gas turbine, its purpose, and, in a reheat gas turbine, whether the combustor is the primary or secondary combustor. Specifically, for reheat engines like the Alstom GT24/GT26, relevant pressures can range from 1 to 30 atm, primary burner inlet temperatures from 700 to 800 K, and secondary inlet temperatures from 1100 K to 1300 K. Flame temperatures typically vary from 1600 to 2200 K and depend mostly on the desired equivalence ratio of the fuel-air mixture (Brower et al., 2012). This large array of relevant conditions drives the need for wide-ranging reactivity studies.

2.2 Natural Gas Ignition Delay Time

Natural gas is mainly composed of methane with varying levels of higher-order hydrocarbons, typically ethane, propane, butane, and pentane. The exact composition of a certain natural gas depends on both the geographic location from where it is extracted and the season during which it is extracted (de Vries and Petersen, 2007). Therefore, it is important to understand the ignition delay time behavior of each constituent and the effect of different levels of a constituent in a natural gas mixture.

For most natural gases, ethane and propane are more than 1% by volume, and butane and pentane are less than 1% by volume (Spadaccini and Colket, 1994). Although methane usually comprises at least 80% of the total volume of the fuel mixture, small levels of higher-order hydrocarbons can dramatically change the ignition delay time of the fuel. This dramatic effect on reactivity is due to the chemical bonding in hydrocarbons. Methane consists of primary carbon-hydrogen bonds which are stronger than the secondary and tertiary bonds in higher-order hydrocarbons. This difference in bond energies allows the decomposition of higher-order hydrocarbons to occur more rapidly than methane. Additionally, decomposition of methane forms methyl, which is a more-stable radical than the radicals formed from the decomposition of higher-order hydrocarbons (Spadaccini and Colket, 1994). Therefore, even after radicals are formed from methane, the time required to break subsequent bonds is longer. Ignition delay time is dependent on the time it takes to produce intermediate species, which then rapidly react to form products (Turns, 2000) Therefore, because the bonds of the higher-order hydrocarbons are easier to break, intermediate species are easier to form, and ignition of the fuel occurs with a shorter delay time.

The ignition delay times of each individual hydrocarbon (C_1-C_5) have been extensively studied. However, the primary focus of this section is the affect that addition of higher-order hydrocarbons has on methane combustion. Mixtures of methane with higher-order hydrocarbons have been studied at a wide range of equivalence ratio, pressure, and

temperature. Most studies have primarily focused on developing correlations for ignition delay time of the form of Eqn. 1.

$$\tau_{ign} = A[HC]^x[O_2]^y exp\left(\frac{E}{RT}\right) \quad (1)$$

Here, A is an empirically determined correlation constant, x and y are empirically determined correlation exponents, E is the activation energy, R is the universal gas constant in kcal/K-mol, and T is the temperature in K. The molar concentration (mol/cm^3) of each species is represented as [i], where i is the species. For this example case, the hydrocarbon used in the correlation is represented as *HC*, and this can be any hydrocarbon of interest (i.e. methane, ethane, propane, etc.). The concentration for each species is found using Eqn. 2. The exponents x and y represent the dependence of ignition delay time on each species' concentration and are found using a linear regression of the data. When additional species are added to a mixture, like a diluent or another hydrocarbon, the equation is multiplied by the species' molar concentration which is raised to a different exponent.

$$[i] = {}^{x_i P}/_{RT} \quad (2)$$

In this equation, i is the species of interest, x_i is the mole fraction of the species in the mixture, P is the pressure in kPa, R is the universal gas constant in cm^3-kPa/K-mol, and T is temperature in K.

Spadaccini and Colket (1994) used an extensive list of previous ignition delay time experiments to develop correlations for methane-air, methane-oxygen, and methane-

hydrocarbon mixtures. They found that the activation energy for methane-hydrocarbon mixtures was slightly less than that for pure methane mixtures. Therefore, mixtures that contained higher-order hydrocarbons required less energy for ignition to occur. Additionally, the exponent for the concentration of higher-order hydrocarbons in the mixture was found to be negative, indicating that as the concentration of higher-order hydrocarbons in the mixture increases, the ignition delay time of the mixture decreases. Huang et al. (2003) examined methane ignition delay time at higher, engine-relevant pressures. As expected, it was found that methane ignition delay times decreased as pressure was increased from 16 to 40 atm. This effect was more noticeable at lower temperatures than higher temperatures due to a reduction in activation energy.

Ethane and propane are most commonly the second and third largest components of natural gas. Due to this level of importance, the ignition delay times of methane/ethane and methane/propane mixtures have been studied extensively. Petersen et al. (2007-a) studied lean mixtures of methane with up to 30% ethane at elevated pressures. It was also found that the addition of ethane to the mixture had an exponential effect: the addition of 10% ethane was found to increase the ignition delay time by a factor of 3, while the addition of 30% ethane was found to increase the ignition delay time by a factor of 10. The effect of propane addition to methane mixtures was explored at elevated pressures for a range of equivalence ratios (Petersen et al. (2007-b). Mixtures that contained up to 40% propane showed that for different temperatures, pressures and equivalence ratios, ignition delay time consistently decreased with increased propane in

the mixture. These results were confirmed when atmospheric tests of methane/ethane and methane/propane were performed by Holton et al. (2010). With less than 10% addition of ethane or propane to methane, ignition delay times noticeably decreased. Ethane was seen to decrease the ignition delay time of the methane-based mixture more than the same amount of propane. Moreover, a significant increase in ignition delay time was found when small amounts of methane were added to ethane or propane. When all three fuels were mixed together, mixtures with the least methane had the shortest ignition delay times.

Butane and pentane are the next most-common constituents found in natural gas. An early study by Higgins and Williams (1969) looked at the addition of small amounts of *n*-butane (hereafter referred to as butane) to methane at an equivalence ratio of 0.5 and sub-atmospheric pressures. They found that the addition of even small amounts of butane to the mixture decreased the ignition delay time significantly. For mixtures with 1 to 3.7% of butane addition, the ignition delay time decreased by a factor of 6, and for mixtures with 12.5% butane addition, the ignition delay time decreased by a factor of 10. This result shows that even small levels of butane can have an important effect on the ignition delay time of a mixture at these conditions. To study the effects at gas turbine-relevant conditions, Healy et al. (2010-a) recently extended the methane/butane ignition delay time database to include higher pressures (10 and 20 atm) and mixtures with higher levels of butane (10 and 30% butane). Addition of 10% butane was seen to increase the mixture reactivity by a factor of 5 over pure methane at both pressures.

Furthermore, the addition of 30% butane was shown to increase the mixture reactivity by an additional factor of 2 over the reactivity of the mixtures with 10% butane at both pressures.

Mixtures of methane and pentane have not been extensively studied in the literature. Crossley et al. (1972) examined one methane/pentane mixture with a low level of pentane and found that the results were similar to those found with the same level of butane. Although there is a lack of methane-pentane data, several studies have examined natural gases containing pentane. Extensive ignition delay time studies have been performed fcrossor two synthetic natural gases with less than 82% methane, NG2 and NG3. The compositions of these two natural gases from Bourque et al. (2010) are shown in Table 1. Experiments over a wide range of pressures showed that ignition delay times increased by a factor of 5 from pure methane to NG2 or NG3. Ignition delay times of NG3 were also lower than those of NG2; however the effect was not as dramatic as the decrease from pure methane. Additionally, experiments over a range of equivalence ratios showed that at lower temperatures and higher pressures, rich mixtures of NG2 and NG3 have shorter ignition delay times than lean mixtures, and at higher temperatures and lower pressures, the opposite is true.

Table 1 Composition of two synthetic natural gases, in volume percent.

Species	NG2 (%)	NG3 (%)
CH_4	81.25	62.5
C_2H_6	10.00	20.0
C_3H_8	5.00	10.0
n-C_4H_{10}	2.50	5.0
n-C_5H_{12}	1.25	2.5

2.3 Hydrogen Ignition Delay Time

The ignition delay time of hydrogen exhibits a counterintuitive dependence on temperature and pressure. This behavior is due to a well-known competition between two initiation reactions in the H_2-O_2 system: the termolecular reaction $H + O_2 + M \rightleftarrows HO_2 + M$ dominates at higher pressures and lower temperatures, while the more-reactive branching reaction $H + O_2 \rightleftarrows OH + O$ dominates at lower pressures and higher temperatures (Law, 2006).

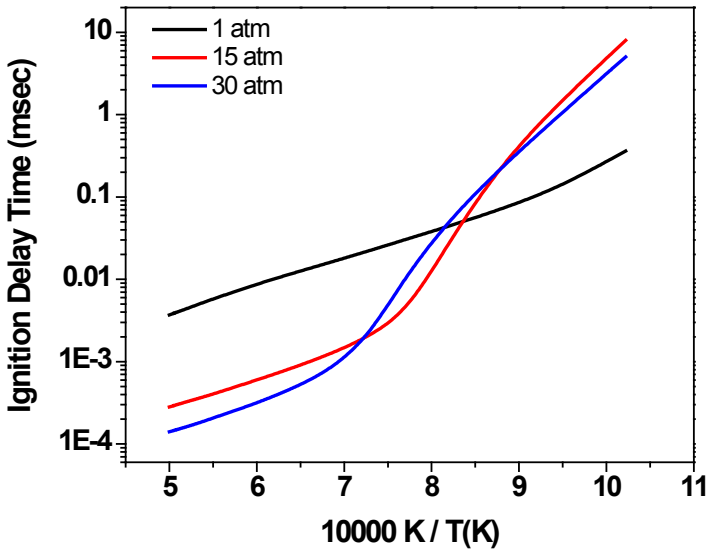

Figure 2 Ignition delay time of stoichiometric hydrogen at various pressures. Adapted from Brower et al. (2012).

This counterintuitive effect of hydrogen chemistry on ignition delay time is shown in Figure 2. At higher temperatures, hydrogen has a higher ignition delay time at 1 atm than at higher pressures. However, at lower temperatures, hydrogen has a lower ignition delay time at 1 atm than at higher pressures. For the conditions studied by Brower et al. (2012), the transition between the two regimes for the higher pressures is seen to occur between about 1250 and 1400 K. Above 1400 K, the $H + O_2 + M \rightleftarrows HO_2 + M$ reaction dominates, indicated by the lower reactivity (longer ignition delay times) at higher pressures.

Research into the ignition delay time of hydrogen has been extensive. Cheng and Oppenheim (1984) performed studies of both methane-oxygen and hydrogen-oxygen

mixtures at low pressures (1 to 3 atm) and formulated correlations similar to Eqn. 1 for both fuels. They found that, for these low pressures, hydrogen had an activation energy that was a factor of two less than the activation energy of methane. This lower activation energy indicates that hydrogen has a much smaller ignition delay time than methane at the same temperature. Herzler and Nuamann (2009) looked at hydrogen ignition delay times at 1, 4, and 16 atm at equivalence ratios of 0.5 and 1. The expected pressure dependence of hydrogen ignition delay time was observed for these mixtures. The transition temperature range at 16 atm was found to be around 1100 K for stoichiometric mixtures and around 1000 K for mixtures with an equivalence ratio of 0.5. This trend shows that the transition between the dominant reactions is also affected by the equivalence ratio of the mixture.

Recently, the ignition delay time of hydrogen at gas turbine-relevant conditions was studied by Fleck et al. (2012). Using a generic reheat gas turbine, ignition delay time of hydrogen in air was studied at a constant pressure of 15 atm with variations in inlet temperature of the combustor and velocity of the H_2/air mixture into the combustor. It was found that temperature dominated changes in ignition delay time for the mixtures, especially at higher inlet velocities. Ignition of hydrogen within the burner was also observed to be independent of the overall equivalence ratio of the mixture in the reheat combustor. Therefore, for a constant pressure, temperature is the most significant factor when looking at ignition delay times of hydrogen mixtures.

Slack (1977) examined data from previous studies and showed that the ignition delay time predicted by kinetics models is heavily dependent on the reaction rates used for the two competing reactions. Due to this large impact of reaction rate values, updates to the H_2-O_2 sub mechanism of hydrocarbon kinetics mechanisms have been continuously carried out as more experimental data become available. Although the present study does not attempt to provide an update to the chemical kinetics mechanism, it is important to note that the hydrogen chemistry in the mechanism used for this study (discussed in greater detail later) has been validated to capture the correct behavior between the two competing reactions. Recently, Ó Conaire et al. (2004) examined data over wide temperature, pressure, and equivalence ratio ranges to provide an update to the chemical kinetics mechanism described later. By performing sensitivity analyses on the reaction rates of the H_2-O_2 system, the mechanism was refined to provide reasonable agreement between the mechanism predictions and experimental ignition delay times of hydrogen.

2.4 Natural Gas/Hydrogen Mixture Ignition Delay Time

For mixtures of natural gas and hydrogen, the primary concern is to understand the level of hydrogen addition at which the mixture is more dependent on hydrogen reactivity than on hydrocarbon reactivity. However, few studies have been performed on the ignition delay time of natural gas-hydrogen mixtures, especially at elevated pressures.

There have been a few studies of the effect of hydrogen addition to methane. Cheng and Oppenheim (1984) looked at eleven different methane-hydrogen mixtures at 1 to 3 atm.

These mixtures varied in equivalence ratio and ranged from pure methane to pure hydrogen. As expected, methane-hydrogen mixtures were always found to have shorter ignition delay times than pure methane and longer ignition delay times than pure hydrogen. A correlation, represented by Eqn. 3, was suggested for methane-hydrogen mixture ignition delay times dependent on the amount of hydrogen in the fuel mixture and the ignition delay times of methane and hydrogen.

$$\tau_{mix} = \tau_{CH_4}^{(1-\varepsilon)} \tau_{H_2}^{\varepsilon} \tag{3}$$

In this correlation, τ_i is the ignition delay time of species *i*, and ε is the mole fraction of hydrogen in the mixture.

Fotache et al. (1997) examined ignition delay times of methane mixtures up to 60% hydrogen heated by air in a counter-flow reactor. They observed that ignition delay time was decreased with the addition of hydrogen to the mixture primarily because of kinetic interactions between methane and hydrogen. Hydrogen radicals that form at the initiation of combustion promote the formation of methyl radicals. More recently, Huang et al. (2006) examined methane-hydrogen mixtures of up to 35% hydrogen at pressures of 16 and 40 atm. It was observed that the difference between ignition delay times of pure methane mixtures and mixtures containing hydrogen was more dramatic at 16 atm than at 40 atm. For a constant pressure, the differences in ignition delay time between mixtures containing hydrogen and pure methane became less noticeable as temperature decreased. Additionally, it was noted that differences between pure methane and

mixtures containing 15% hydrogen were much less significant than differences seen between pure methane and mixtures containing 35% hydrogen.

Zhang et al. (2012) have recently extended the ignition delay time database for methane-hydrogen mixtures by examining reactivity of 0-100% hydrogen fuel mixtures at pressures from 5 to 20 atm. Typical hydrocarbon ignition delay time behavior, i.e. decreasing ignition delay time with increasing pressure, was observed when the fuel mixture was less than 40% hydrogen. From 40 to 60% hydrogen, a linear regression showed the exponent of pressure trending to zero, indicating that the ignition delay time has a negligible dependence on pressure. When hydrogen was 80% of the mixture, the complex nature of hydrogen reactivity dominated the ignition delay time of the fuel mixture. For this mixture, at high temperatures, the ignition delay time decreased significantly with an increase in pressure; at intermediate temperatures, the opposite pressure dependence was found, and at low temperatures, there was no pressure dependence exhibited. Additionally, it is shown that although hydrogen is the major component in the 20%CH_4/80%H_2 mixture, the reactivity of pure hydrogen has a noticeably different pressure dependence.

Fewer studies have been performed for natural gases with higher order hydrocarbons. A study by Herzler and Nuamann (2009) looked at the effect of hydrogen addition to natural gas modeled as 92% methane and 8% ethane. They looked at mixtures with 0 to 100% hydrogen at pressures of 1, 4, and 16 atm and equivalence ratios of 0.5 and 1.

Overall, the addition of ethane to the mixtures, and the subsequent reduction of methane, caused a decrease in the ignition delay times. The ignition delay times were seen to have linear dependence on temperature and pressure until hydrogen was 80% of the mixture, similar to the methane-hydrogen mixtures seen by Zhang et al. (2012).

A recent study by Brower et al. (2012) contained flame speed and ignition delay time calculations for pure methane and NG2 (described in Table 1) with 0 to 100% hydrogen. A parametric study was performed for ignition delay times at conditions relevant for the secondary burner of a reheat gas turbine. As pressure was varied from 1 to 30 atm, the effect of hydrogen addition to the base hydrocarbon was observed. Figure 3, adapted from Brower et al. (2012), shows the results from the parametric study at a temperature of 1100 K and an equivalence ratio of 0.7. For both methane and NG2, the ignition delay times appear to linearly decrease as pressure increases until about 70% hydrogen is added. At 70% hydrogen addition and 90% hydrogen addition, the hydrocarbon fuels are seen to start adapting to the pressure dependence seen in the pure-hydrogen case. The results were similar at an inlet temperature of 1300 K and equivalence ratio of 0.7 as well as at an inlet temperature of 1100 K and an equivalence ratio of 1.1. The last two calculations also show slight increases in ignition delay times for higher equivalence ratios and slight decreases in ignition delay times at higher inlet temperatures.

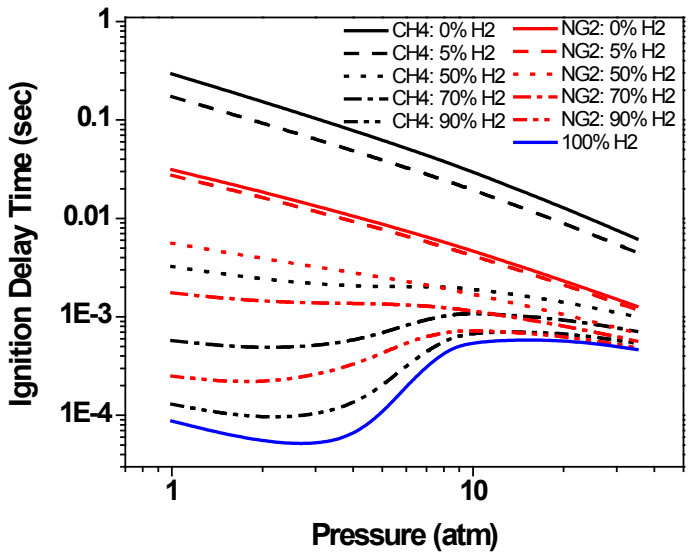

Figure 3 Ignition delay times of methane and NG2 with 0 to 100% hydrogen addition at an inlet temperature of 1100 K and an equivalence ratio of 0.7. From Brower et al. (2012).

Brower et al. (2012) also developed a gas turbine model using the chemical kinetics solver CHEMKIN (Reaction Design, Inc., 2011). This model calculated laminar flame speeds based on conditions in the primary burner and ignition delay times based on conditions in the secondary burner. In Figure 4, the normalized ignition delay times of methane and NG2 are plotted as a function of hydrogen addition for three different pressures, 1, 15, and 30 atm. One can see from this figure that the ignition delay time of a hydrocarbon decreases dramatically with the addition of hydrogen. At 15 atm, the ignition delay time decreases by almost two orders of magnitude from pure methane to pure hydrogen. The effect is less dramatic with NG2 since pure NG2 has a shorter ignition delay time than pure methane. Additionally, the effect of hydrogen addition decreases as pressure increases.

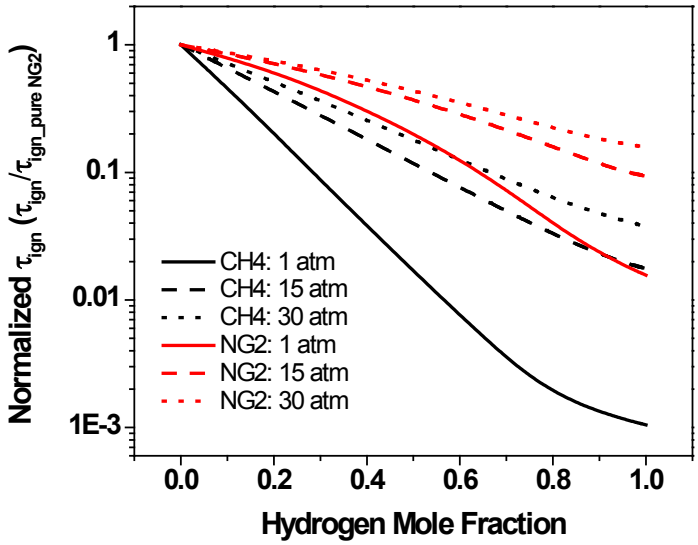

Figure 4 Ignition delay time of mixtures of methane and NG2, plotted as a function of hydrogen mole fraction. Values are normalized to the ignition delay time of pure NG2 at each pressure. From Brower et al. (2012).

The studies highlighted above and the calculations performed by Brower et al. (2012) highlight the need for further experimental studies. Although the study by Brower et al. (2012) was extensive, there is still a lack of experimental data for natural gases with high levels of hydrogen, especially at gas turbine-relevant conditions. The need for the experimental validation of these calculations led to the study to follow.

CHAPTER III

EXPERIMENTAL SETUP

3.1 Shock-Tube Facility

Experiments were performed in the high-pressure shock-tube facility described in detail by Aul (2009) and shown in Figure 5. The shock tube is made entirely of 304 stainless steel. The driven section is 4.72-m long with an internal diameter of 15.24 cm, and the driver section is 2.46-m long with an internal diameter of 7.62 cm. The large diameter of the driven section allows for experiments to be performed with minimal boundary layer effects. The length of the shock tube allows the observation of ignition delay times of up to 2 msec before any significant pressure drop is observed.

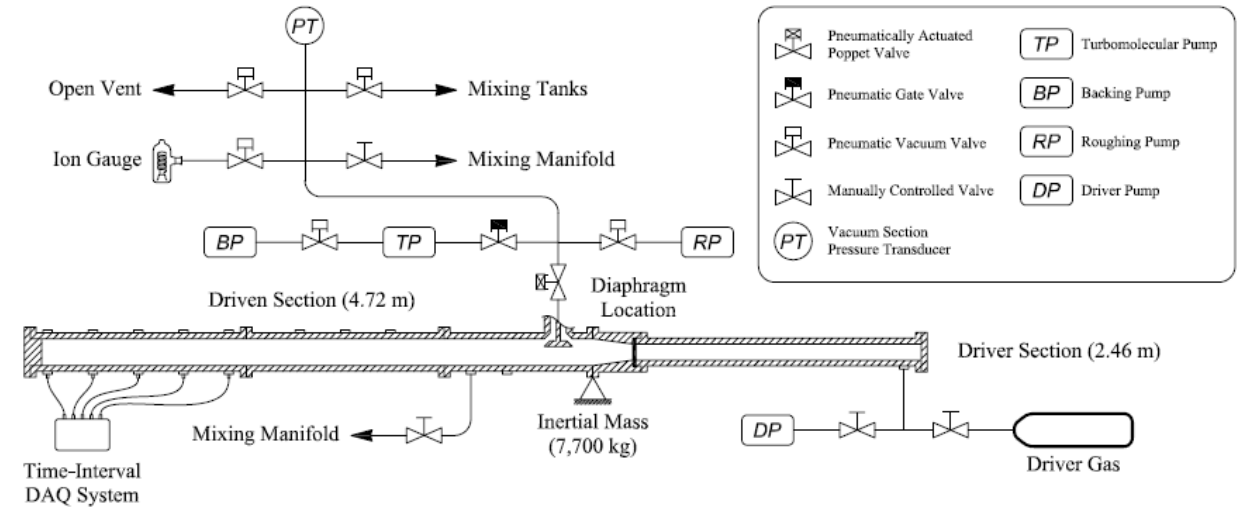

Figure 5 Schematic drawing of high-pressure shock-tube facility from Aul (2009).

The inner diameter of the driver section is expanded to the driven section inner diameter through a diverging section located directly after the diaphragm location. The easy

accessibility of the diaphragm section allows for experiments at different pressures to be performed in the same shock tube. The diaphragms used herein were different for each of the three pressures. For 1 atm experiments, polycarbonate diaphragms with widths of 0.01″ were used. To achieve test conditions as close as possible to 10 atm, several polycarbonate diaphragms with widths of 0.04″, 0.01″, and 0.005″ were used. Typically, the experiments were performed with one 0.04″ diaphragm, two 0.01″ diaphragms, and one 0.005″ diaphragm, but this varied depending on the mixture and temperature of the experiment to stay within ±0.5 atm of 10 atm. For 30-atm experiments, prescored aluminum diaphragms with widths of 0.09″ were used. The experimental pressures for the 30atm experiments varied by about 3 atm between mixtures due to slight differences in batches of aluminum diaphragms.

Helium was used as the driver gas, and the driver section was filled slowly until the diaphragm burst to ensure repeatability between experiments. Ultra-high purity (UHP, 99.9995%) gases were used to make the test mixtures containing Ar, O_2, CH_4, C_2H_6, C_3H_8, *n*-C_4H_{10}, *n*-C_5H_{12}, and H_2. The two natural gases used in the study, shown in Table 1, were each prepared separately to ensure repeatability with the natural gases used. The natural gases were prepared using the partial pressure method in tanks that were vacuumed down below 1×10^{-7} torr. The partial pressure of pentane was kept well below the vapor pressure of pentane to ensure that it was always in the gaseous phase and well mixed in the natural gas mixtures. The natural gas mixtures were prepared and allowed

to sit at least 24 hours before they were used to make the fuel-oxidizer-diluent mixtures for the experiments.

After the natural gas mixtures were prepared, the mixtures from the test matrix were made. All mixtures from the L9 test matrix (described later) were diluted in 90% argon. Each mixture was made in a mixing tank connected to the shock tube using the partial pressure method. The mix tank was vacuumed to pressures below 10^{-6} before each mixture was made. The gases were introduced to the mix tank through a perforated stinger to create turbulent mixing. In addition, each constituent was slowly added to the mix tank to ensure proper mixing.

The conditions at which the combustion event occurs are dictated by the conditions behind the shock wave after it is reflected off the endwall of the driven section of the shock tube. These conditions are dependent on the incident shock wave velocity, the initial fill conditions of the driven section, and the properties of the gas in the driven section. For the shock tube used herein, incident-shock velocity in the test region was found using five, PCB 113 pressure transducers in series along the shock tube. These pressure transducers sent signals to four, Fluke PM 6666 time-interval counters that output the time intervals that were seen by the pressure transducers as the shock wave passes. These four time intervals and the distances between the pressure transducers were then used to find the velocity of the incident shock wave. Using this velocity and the standard one-dimensional shock relations that incorporate the fill conditions and

properties of the gas in the driven section, conditions behind the reflected shock wave for each experiment was calculated. Petersen et al. (2005) showed that this method is highly reliable and determines reflected-shock temperatures that are within ± 10 K of the actual temperature.

Within a shock tube, ideal ignition is an event that begins at the endwall sometime after the reflected shockwave has passed and then travels upstream. The time between when the reflected shockwave initially passes and when the ignition event begins is defined as the ignition delay time (τ_{ign}). It is ideal to measure the ignition event from the endwall using the endwall pressure signal, as depicted in Figure 6. In this case, the combustion event is exothermic enough to produce a significant and measurable rise in pressure.

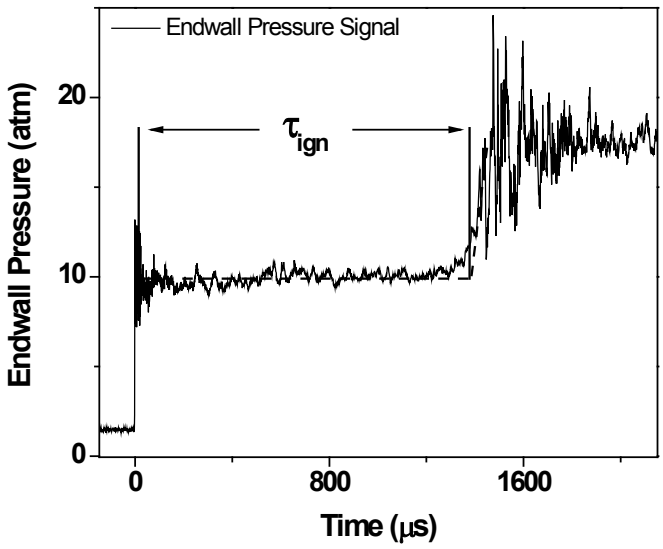

Figure 6 Ignition delay time measurement from endwall pressure signal. Experiment shown was performed mixture of NG3 and 30% H_2 with an equivalence ratio of 1 at conditions of 9.6 atm and 1199 K.

In the present study, all mixtures were diluted in 90% argon and, due to this dilution, some of the mixtures used were not exothermic enough at all conditions to produce a strong pressure rise at the endwall. In these few cases, the sidewall OH(A→X) (hereafter referred to as OH*) emission was used to determine the ignition delay time, as shown in Figure 7. The beginning of the ignition delay time was defined by the sidewall pressure signal, and ignition was indicated by the rise in OH* emission. The ignition delay time found from the sidewall OH* signal was preferred to the ignition delay time found from the endwall OH* emission signal. This preference is because in dilute mixtures, using the endwall emission to determine the ignition delay time can result in artificially long ignition delay times (Petersen, 2009).

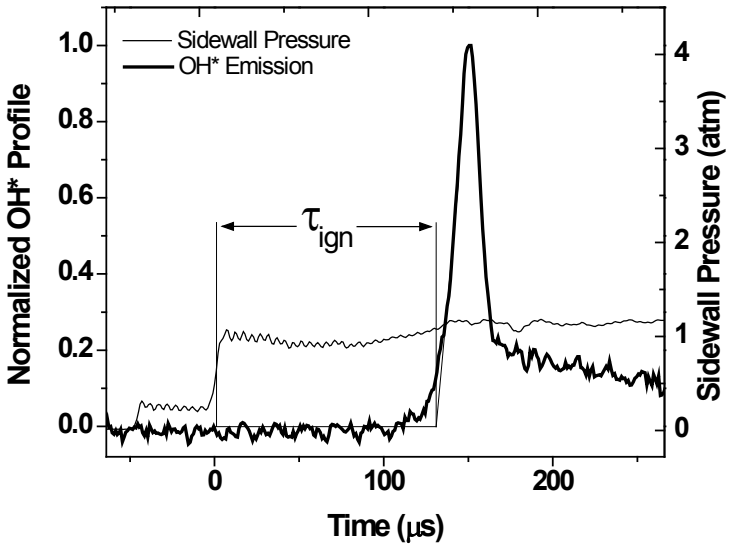

Figure 7 Ignition delay time measurement from OH* emission signal. Experiment shown was performed mixture of CH_4 and 30% H_2 with an equivalence ratio of 0.3 at conditions of 1.5 atm and 1645 K.

3.2 Experimental Uncertainty

Experimental uncertainty in ignition delay time measurements is due to several aspects of the experiment. First, the method of determining the reflected-shock conditions is known to be accurate to ± 10 K. At an average temperature of 1250 K for all mixtures performed, this indicates about 2% uncertainty is added to the ignition delay time data due to possible variations in temperature.

The mixture production method, although fairly accurate, can add some uncertainty to the data as well. In 90% argon, the fuel constituents were at partial pressures on the order of 100s of torr. The accuracy of the pressure gage that determined the pressure of the mixture as these constituents were added was to 10^{-1} torr. Additionally, the oxygen was usually at a pressure above the limit of the vacuum pressure gage and was therefore added to the mixture using a psi-based pressure gage. This pressure gage was accurate to 10^{-1} psi. Argon was the last constituent added to the mixture and was added to the mixture using the psi pressure gage. Overall, the mixture process and the accuracy of the pressure gages add about 1% uncertainty to the ignition delay time of a specific mixture.

The method of determining ignition delay time also introduces a level of uncertainty to the calculations. Since these calculations are performed graphically and are open to interpretation (when choosing which feature(s) on which to base the ignition event), the uncertainty is mostly due to human error. Repeat calculations of ignition delay time measurements from the same experiment are generally within 5% of each other.

All of these factors introduce uncertainty to the ignition delay time measurements. Additionally, there are slight uncertainties from experiment to experiment due to differences in the diaphragm bursting, signals from the diagnostics, and other minor experimental factors. Due to all of these factors, the overall uncertainty of an ignition delay time was determined to be 10%.

3.3 Chemical Kinetics Model

The most recent chemical kinetics model from the National University of Ireland, Galway, was compared to all experiments. This kinetics model is under constant development at the Combustion Chemistry Center and describes the combustion chemistry up to C_5 (http://c3.nuigalway.ie/naturalgas3.html, 2010). This chemical kinetics mechanism is based on the hierarchical nature of combustion kinetics. The basic sub-mechanism is comprised of the $H_2/O_2/CO$ chemistry that has recently been updated based on experimental and kinetics data (Ó Conaire et al., 2004). The C_1-C_3 sub mechanism has also been under constant development, with the most recent updates described by Metcalfe et al. (2011). Some important saturated species, like 1,3-butadiene, propene, and various alkenes, have been added to the mechanism based on work by Davis et al. (1999) and the mechanism developed by Laskin et al. (2000). Recent developments for the butane and pentane mechanism are described by Healy et al. (2010-b).

In addition to this chemical kinetics mechanism, the OH* mechanism developed by Hall and Petersen (2005) was used to define ignition delay times of each calculation. Using the chemical kinetics solver CHEMKIN (Reaction Design, Inc., 2011), the complete kinetics model was used to predict the chemistry at each specific experimental condition. The OH* profile from each simulation was used to find the predicted ignition delay time of the mixture at those conditions, as shown in Figure 8.

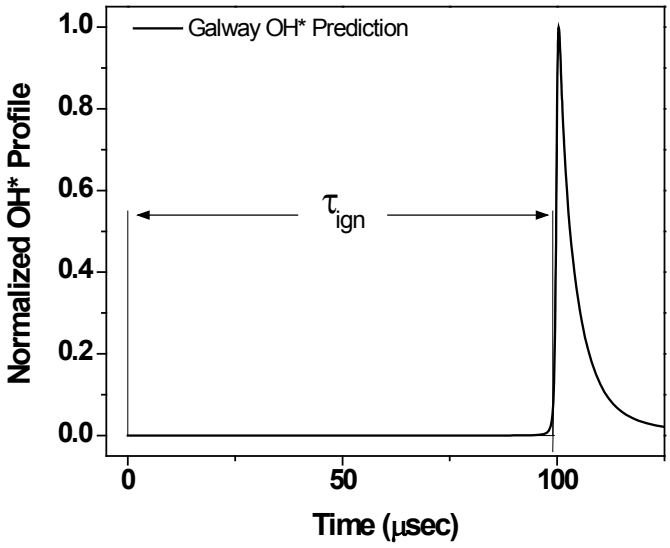

Figure 8 Ignition delay time measurement from Galway OH* prediction. Prediction shown was performed with a mixture of CH_4 and 30% H_2 with an equivalence ratio of 0.3 at conditions of 1.5 atm and 1645 K.

3.4 Experimental Matrix

The effect of hydrogen addition to methane and natural gas has been shown to vary with the amount of higher-order hydrocarbons in the natural gas, the equivalence ratio, and the pressure. A test matrix was developed to test these different aspects in an organized

matter. Three baseline natural gases were used: pure methane, NG2, and NG3. From previous studies (Brower et al., 2012), it was determined that three levels of hydrogen addition would be sufficient to capture the key effects of different levels of hydrogen addition. Thirty percent hydrogen addition was chosen to test the effect of a low level of hydrogen that, in chemical calculations, was predicted to not affect the linear pressure dependence expected for a hydrocarbon. Sixty percent hydrogen addition was tested to determine if the reactivity would still have the linear pressure dependence even when more than half of the fuel mixture is hydrogen. Finally, 80% hydrogen addition was examined to determine the effect of a low level of natural gas on hydrogen reactivity. Since it was observed previously (Brower et al., 2012) that the equivalence ratio could play a small role on ignition delay time of a mixture, three equivalence ratios were chosen for the experiments (0.3, 0.5, and 1). The pressure was also varied from 1 to 30 atm to test the pressure dependence of these mixtures.

Three levels of each variable were assembled into the L9 Taguchi array (Ross, 1988), shown in Table 2. The specific mole fractions of NG2 and NG3 are listed in Table 1, and the specific mole fractions for each combination are listed in the appendix. Experiments were performed for each combination at the designated pressure and at 9 - 14 different temperatures. The temperature ranges were varied to obtain ignition delay times from around 100 μs to 2 ms for each combination.

Table 2 L9 test matrix developed using the Taguchi method for balanced, orthogonal arrays. Three levels of each factor were used.

Combo	Fuel	$\%H_2$	ϕ	P (atm)
1	CH_4	30	0.3	1
2	CH_4	60	0.5	10
3	CH_4	80	1	30
4	NG2	30	0.5	30
5	NG2	60	1	1
6	NG2	80	0.3	10
7	NG3	30	1	10
8	NG3	60	0.3	30
9	NG3	80	0.5	1

CHAPTER IV

RESULTS

Experiments were performed for each of the 9 combinations at the designated pressure and at least nine different temperatures. The temperature ranges were varied to obtain ignition delay times from around 100 μs to 2 ms for each combination. The experimental data and conditions are listed for each combination of the L9 matrix in the appendix. The experimental ignition delay times were compared to ignition delay times predicted by the Galway mechanism. This comparison between the model and the experimental results shows areas where the model performs well and where improvement of the model could be implemented. The datasets are presented in the order of the experimental matrix. After each three combinations from the same base natural gas (i.e. methane, NG2, or NG3), the three combinations are plotted together to draw further conclusions. All ignition delay times are plotted on a base 10-logarithmic scale as a function of the inverse of the temperature.

Ignition delay time data for combination 1 are presented in Figure 9. The temperature range for this combination was 1283 K to 1722 K. It is shown later that this was one of the least reactive combinations and therefore had the highest temperature range of all combinations. This lower reactivity was expected since combination 1 contained the maximum amount of methane at the lowest pressure possible. The Galway model predicted ignition delay times that were an average of 31% higher than the experimental data. However, the model appears to accurately predict the trend of linearly decreasing ignition delay times with increasing temperature that is seen in the experimental data.

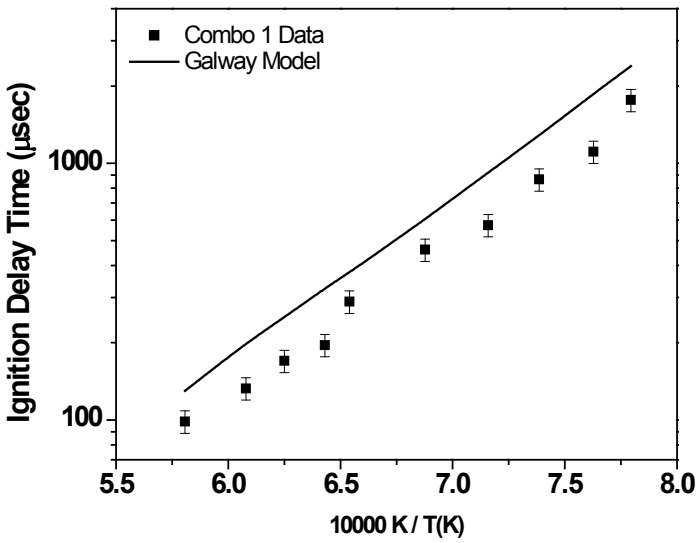

Figure 9 Ignition delay times of 30% H_2 added to pure methane with an equivalence ratio of 0.3 at a pressure of 1 atm are shown. Galway model predictions are also plotted against the data as a line.

The ignition delay time data found for combination 2 are presented in Figure 10 compared to the Galway mechanism at the same conditions. Ignition delay times were taken for a temperature range of 1116 K to 1317 K. The significantly lower temperature range indicates that this combination is more reactive than combination 1 since a similar range of ignition delay times was achieved with lower temperatures. Similar to combination 1, the data are seen to have a fairly linear trend with temperature. The Galway model fairly accurately describes this trend although the model has a slightly nonlinear curve and under predicts the data. This error in the model prediction could be due to an effect of the hydrogen addition, pressure, or equivalence ratio.

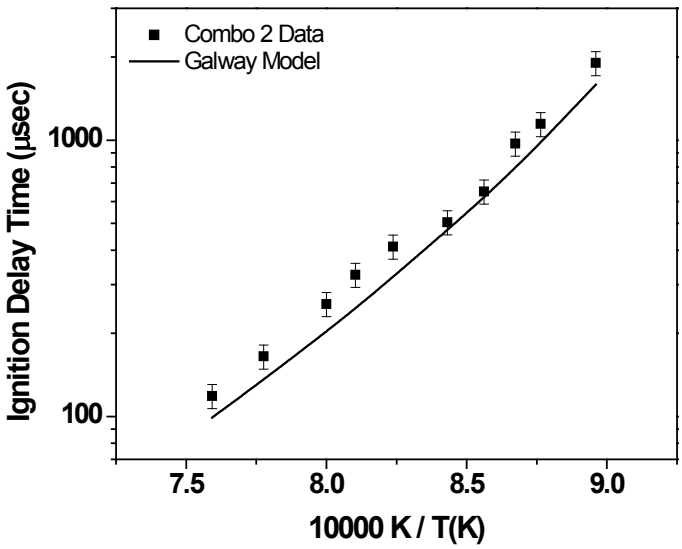

Figure 10 Ignition delay times of 60% hydrogen added to pure methane with an equivalence ratio of 0.5 at a pressure of 10 atm are shown. Galway model predictions are also plotted against the data as a line.

Ignition delay times of combination 3 are presented in Figure 11 compared to the Galway model at the same conditions. For this combination, the temperatures ranged from 1110 K to 1220 K. This range of temperature is the lowest seen between combinations 1 to 3, indicating that this is the most reactive combination for the set of methane combinations. The trend of the data, linearly decreasing ignition delay times with increasing temperature, is captured by the Galway model but the data are under predicted. The Galway model also appears to predict a slightly different slope than slope of the data. This behavior again indicates that the Galway model is incorrectly predicting the effect of hydrogen, pressure, or equivalence ratio on the reactivity at these conditions.

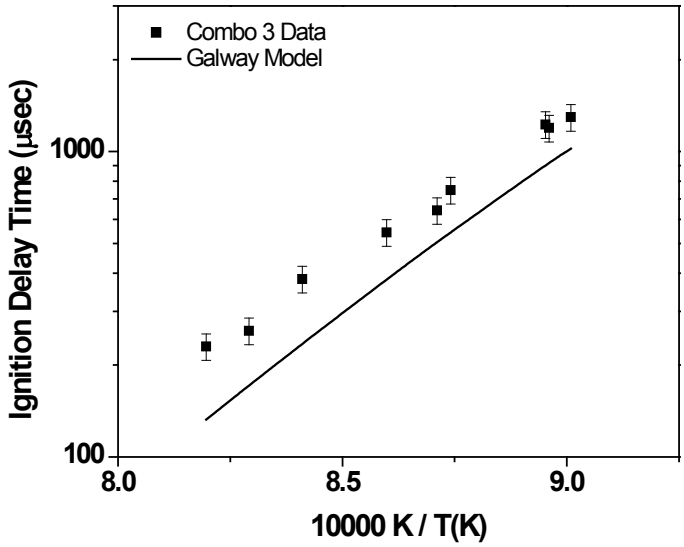

Figure 11 Ignition delay times of 80% hydrogen added to pure methane with an equivalence ratio of 1 at a pressure of 30 atm are shown. Galway model predictions are also plotted against the data as a line.

Ignition delay times for combinations 1, 2, and 3 are plotted in Figure 12. The reactivity appears to increase from combination 1 to combination 2 and then from combination 2 to combination 3. Additionally, combination 1 is much less reactive than both combinations 2 and 3, which are similar in reactivity. The trends all appear to be linear with temperature, both for the data and the Galway models. Combination 3 appears to be the most significantly under predicted combination, while only combination 1 is over predicted by the model. Due to the nature of the experimental matrix, conclusions on which factor influences the reactivity of the methane fuels cannot be made from this information since more than one parameter was changed between each combination.

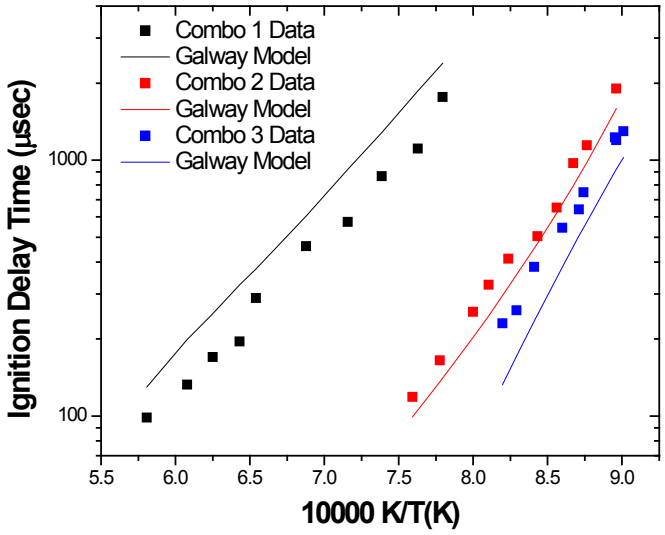

Figure 12 Ignition delay times from the CH_4-based combinations 1 through 3 are plotted as a function of the inverse of the temperature. Galway models for each combination are plotted as lines.

Ignition delay times of combination 4 are presented in Figure 13 compared to the Galway model calculated at the same conditions. Temperatures for the experiments with combination 4 ranged from 1152 K to 1299 K. The data appear to have a linear trend in which ignition delay time increases with decreasing temperature. The Galway model describes the trend of the data fairly accurately. However, the Galway model slightly under predicts the experimental data.

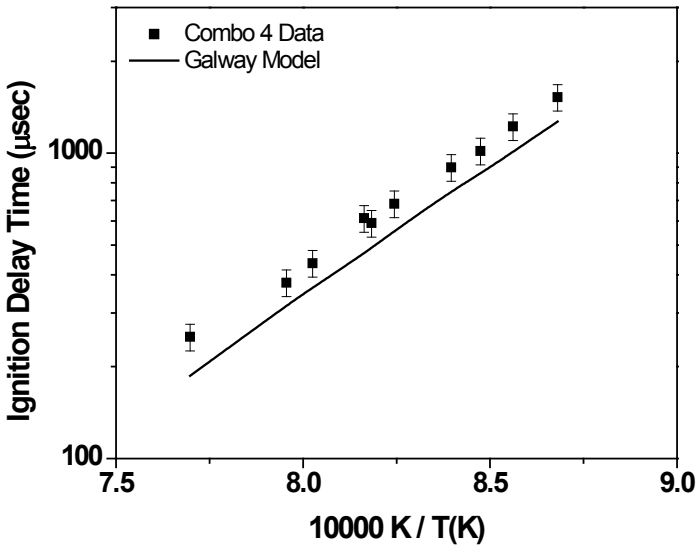

Figure 13 Ignition delay times of 30% hydrogen added to NG2 with an equivalence ratio of 0.5 at a pressure of 30 atm are shown. Galway model predictions are also plotted against the data as a line.

Figure 14 shows the ignition delay times of combination 5 compared to the Galway model at the same conditions. The temperatures for these experiments ranged from 1241 K to 1443 K. The higher temperature range than for the experiments of combination 4 indicates that this combination was less reactive than combination 4. Although there is more hydrogen in this combination, the lower reactivity could be due to the significantly lower pressure or the higher equivalence ratio. The Galway model predicts both the trend and the absolute values of the data within the expected uncertainty at these conditions. Additionally, both the data and model show a linear decrease in ignition delay time with increasing temperature.

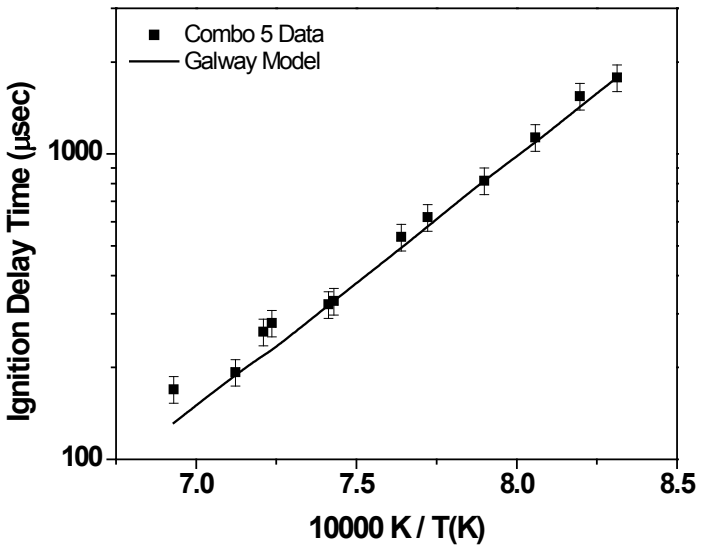

Figure 14 Ignition delay times of 60% hydrogen added to NG2 with an equivalence ratio of 1 at a pressure of 1 atm are shown. Galway model predictions are also plotted against the data as a line.

Ignition delay times for combination 6 are shown in Figure 15 along with the Galway model predictions at the same conditions. The temperature range for this data set is 1101 K to 1196 K. The data decrease linearly from the lowest temperature until about 1150 K. Then, the linear trend of the data changes and the data begin to decrease at a slower rate as temperature increases. The Galway model accurately predicts the lower temperature trend seen in the data but fails to predict the change in the trend seen at 1150 K. This behavior indicates that the model might not accurately predict the effect of hydrogen addition, pressure, or equivalence ratio at these conditions.

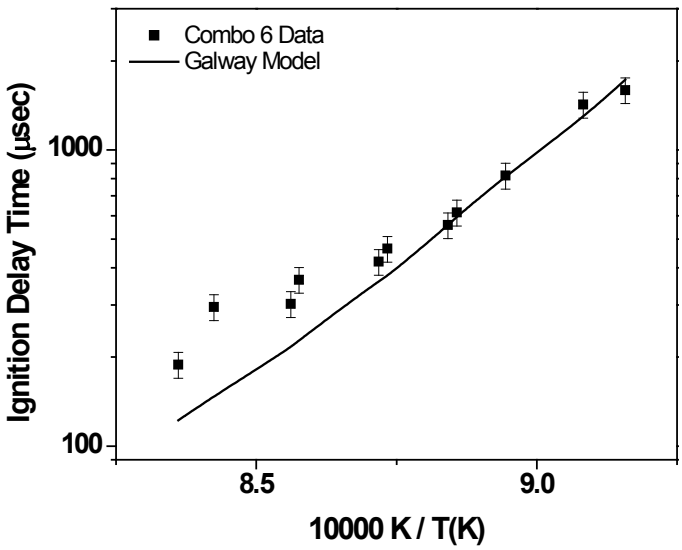

Figure 15 Ignition delay times of 80% hydrogen added to NG2 with an equivalence ratio of 0.3 at a pressure of 10 atm are shown. Galway model predictions are also plotted against the data as a line.

Ignition delay times for combinations 4, 5, and 6 are plotted together in Figure 16. Combination 5 appears to be the least reactive combination while combination 6 is the most reactive. The trends of combinations 4 and 5 appear to be purely linear, while the slope of the linear trend of combination 6 changes around 1150 K. The order of reactivity of the combinations follows decreasing order of equivalence ratio, indicating that equivalence ratio could play a significant role for these combinations. However, since this is not the only factor changing between combinations, a factor sensitivity analysis was performed to find the factor that is playing the most significant role, as shown later. The Galway model does fairly well at predicting the data for these three combinations, although it does not predict the change in the linear trend seen in combination 6.

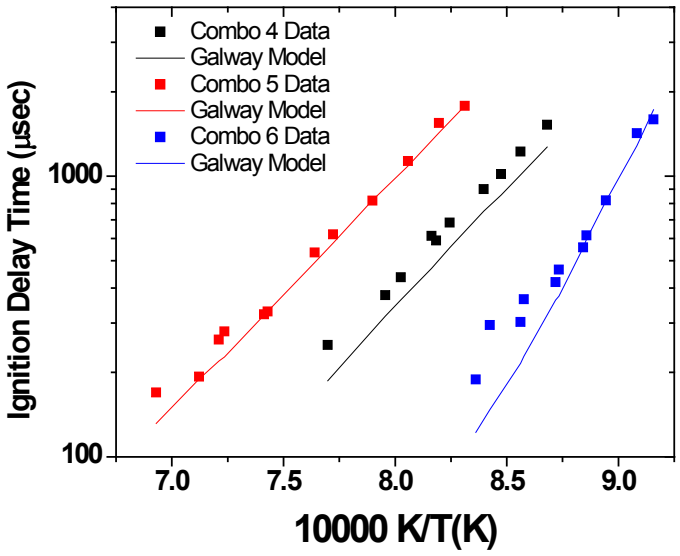

Figure 16 Ignition delay times from NG2-based combinations 4 through 6 are plotted as a function of the inverse of temperature. Galway models for each combination are plotted as lines.

Ignition delay times from combination 7 are plotted as a function of inverse temperature in Figure 17. The experiments were performed in a temperature range of 1192 K to 1381 K. The data appear to follow a linear trend, and ignition delay times decrease with increasing temperature. The Galway model appears to follow a similar trend, although the model under predicts the data. Additionally, the model under predicts the ignition delay times more at higher temperatures.

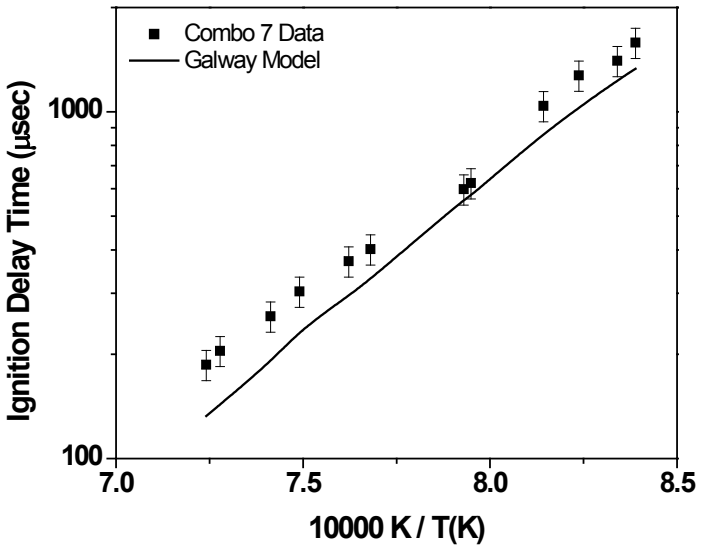

Figure 17 Ignition delay times for 30% hydrogen added to NG3 with an equivalence ratio of 1 at a pressure of 10 atm are shown. Galway model predictions are also plotted against the data as a line.

Figure 18 shows the ignition delay times of combination 8 as a function of the inverse of the temperature. The experimental temperatures for this combination ranged from 1134 K to 1253 K. This temperature range is on the lower end of the temperature range for combination 7, indicating that this combination is more reactive. The data appear to have a linear trend, and the ignition delay times decrease with an increase in temperature. The Galway model predictions show a similar trend but noticeably under predict the data.

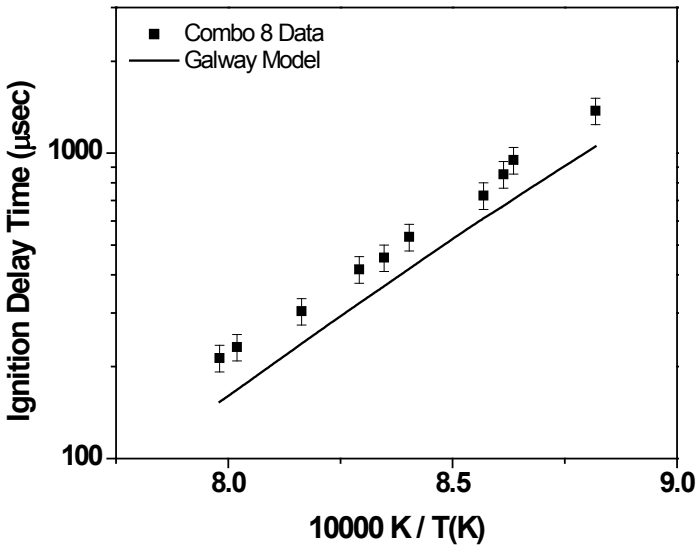

Figure 18 Ignition delay times of 60% hydrogen added to NG3 with an equivalence ratio of 0.3 at a pressure of 30 atm are shown. Galway model predictions are also plotted against the data as a line.

Ignition delay times for combination 9 are plotted in Figure 19 as a function of inverse temperature. The data for combination 9 were found in a temperature range of 1112 K to 1280 K. This temperature range is very similar to that of combination 8, indicating similar reactivity for the two combinations. The data appear to have a mostly linear trend with temperature. The Galway model fairly accurately predicts the linear trend at lower temperatures but predicts a slightly different trend at higher temperatures. The Galway model under predicts the data, and the predictions get worse as temperature increases.

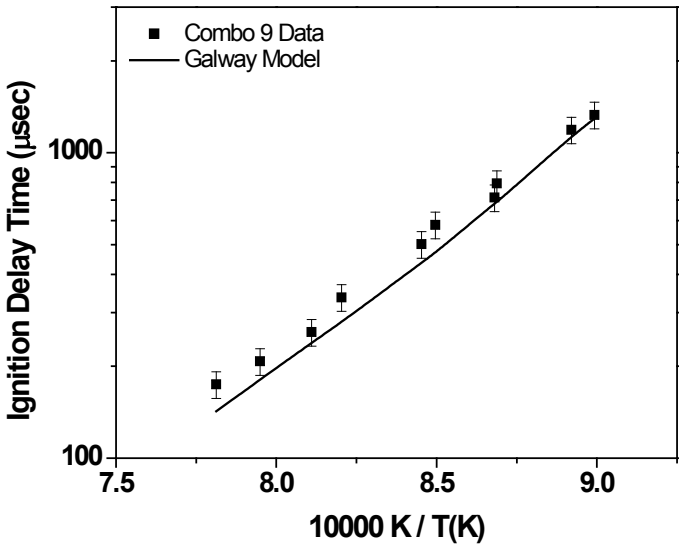

Figure 19 Ignition delay times of 80% hydrogen added to NG3 with an equivalence ratio of 0.5 at a pressure of 1 atm are shown. Galway model predictions are also plotted against the data as a line.

The ignition delay times for all three combinations containing NG3 (combinations 7 through 9) are shown in Figure 20. One noticeable feature seen in this figure is that two of the combinations, 8 and 9, have overlapping ignition delay times. Combination 9 is seen to cross over combination 8. Additionally, combination 7 is seen to be significantly less reactive than the other two combinations. Although the Galway model under predicts all of the data for the NG3 combinations, the trends are very accurately predicted. In the Galway predictions, combination 9 is seen to cross combination 8 and combination 7 is significantly less reactive than the other two combinations.

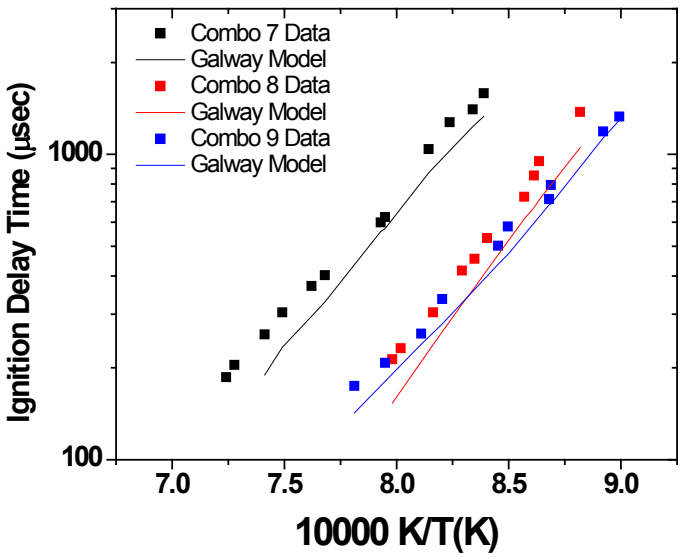

Figure 20 Ignition delay times from NG3-based combinations 7 through 9 are plotted as a function of the inverse of temperature. Galway models for each combination are plotted as lines.

CHAPTER V

DISCUSSION

Further analysis of the results presented in the previous chapter was performed in an attempt to determine which factor (natural gas composition, H_2 content of the fuel mixture, equivalence ratio, or pressure) played the largest role in the ignition delay times of the combinations studied. In this chapter, experimental correlations are developed for each individual combination, each set of three combinations (based on the natural gas of the combination), and for the full L9 matrix. A factor sensitivity is performed on the L9 matrix using the correlations developed for each combination. Then, calculations for all possible combinations for the conditions of the study (the full matrix) are performed, and correlations are developed for L9 matrices for each natural gas. Finally, comparisons are made between correlations from the full factorial matrix and L9 matrices for each natural gas to show the effect of using a reduced L9 matrix for each natural gas.

5.1 Experimental Correlations

To further understand the trends within the data and to provide a means of predicting ignition delay times outside of the data set without the use of the detailed mechanism, correlations were developed. These correlations for each individual combination were developed using Eqn. 4. In this equation, τ_{ign} is the ignition delay time, A is the correlation constant, E is an ignition activation energy of the combination in kcal/mol, R is the universal gas constant in units of kcal/mol-K, and T is the temperature in K.

$$\tau_{ign} = A exp\left(\frac{E}{RT}\right) \tag{4}$$

Three separate correlations were developed for each set of 3 combinations that contained each natural gas (CH_4, NG2, or NG3). These correlations are described in further detail in each subsection for that natural gas below and are generally of the form of Eqn. 5.

$$\tau_{ign} = A[NG]^x[H_2]^y[O_2]^z exp\left(\frac{E}{RT}\right) \quad (5)$$

In Eqn. 5, *NG* indicates the natural gas common to the set of three combinations, *[ ]* indicates the concentration of the species inside the brackets in mol/cm^3, and *x*, *y*, and *z* are empirically derived correlation exponents.

In the following subsections, the correlations are explored further for each subset of natural gas combinations. The correlations are described, and then each data set is plotted with the correlations to compare the correlations together with the data. In the final subsection, an attempt at correlating the entire L9 matrix is discussed. Several correlation schemes are shown and compared to the experimental data.

5.1.1 Methane Combination Correlations

Using Eqn. 4, individual correlations were found for combinations 1 through 3. The values for A and E for each combination are listed in Table 3. The activation energies of the combinations are seen to increase from combination 1 to combination 3. This trend implies increasing reactivity in the combinations, which was seen in the experimental results.

Table 3 Correlation constants and activation energies found for correlations of combinations 1 through 3 individually.

Combo	A	E (kcal/mol)
1	2.42×10^{-2}	28.2
2	4.02×10^{-5}	38.9
3	3.72×10^{-6}	43.4

After the correlations for the individual combinations were found, a correlation for the natural gas set was found. This multiple-combination correlation is described in Table 4.

Table 4 Correlation for combinations 1 through 3.

A	x	y	z	E	R^2
8.09×10^{5}	19.3	-4.71	-15.0	34.2	0.962

Although this correlation has a coefficient of multiple determination, R^2, value above 0.9, the exponents *x*, *y*, and *z* are quite large. Generally, the absolute value of exponents of a correlation of this form should be on the order of 1 or less. Since the exponents in this case are so large, it is possible that some factor, like pressure or equivalence ratio, is over specified. Due to this potentially misleading result, other forms of the correlation were explored using different variables to describe the combinations. The correlation that ultimately gave the most physically realistic exponents was of the form of Eqn. 6.

$$\tau_{ign} = A[CH_4]^x[H_2]^y[Ar]^z\varphi^w exp\left(\frac{E}{RT}\right) \quad (6)$$

In this equation, *x, y, z,* and *w* are the empirically derived correlation exponents that describe the contribution of each aspect on the ignition delay time, and φ is the equivalence ratio of the combination. The new values for the coefficients are listed in Table 5.

Table 5 Correlation for combinations 1 through 3 utilizing Eqn. 6.

A	x	y	z	w	E	R^2
6.37×10^{-9}	0.00	-2.32	1.90	3.13	34.2	0.962

This correlation describes a few features of combinations 1 through 3. First, since the exponent *x* is zero, the effect of the concentration of methane on the reactivity is negligible. This result is likely because changes in the methane concentration are a function of the concentrations of the other species. The negative sign for the exponent that corresponds to the concentration of hydrogen, *y*, indicates that increasing the hydrogen concentration decreases the ignition delay time. This effect of the H_2 was expected as the reactivity of hydrogen is much higher than that of methane. Since the argon dilution was the same for each combination, the effect of the argon concentration can be used as an indication of the effect of the ratio of pressure and temperature. The positive exponent for argon concentration, *z*, implies that as the ratio between pressure and temperature decreases, ignition delay time decreases. Similarly, the positive exponent for the equivalence ratio, *w*, indicates that the ignition delay time decreases as equivalence ratio decreases.

Further information about the accuracy of the correlations can be seen graphically. Figure 21 through Figure 23 show the different combinations plotted with the correlations for each data set. In the appendix, the correlations are compared graphically to the experimental data and plotted against a 1 to 1 line.

In Figure 21, the data from combination 1 are plotted against the Galway model, the correlation developed for combination 1, and the correlation developed for combinations 1, 2, and 3. The correlation for combination 1 lies directly on top of the data, as expected. The data match this correlation generally within the 10% uncertainty expected for the data. The multiple-combination correlation developed using combinations 1 through 3 also shows decent agreement with the data. It performs slightly worse in predicting the general trend seen in the data since the slope of the line appears to be slightly incorrect. If this correlation were used to predict ignition delay times outside of the temperature range that was studied, the predictions would be under predicted for higher temperatures and moderately over predicted for lower temperatures.

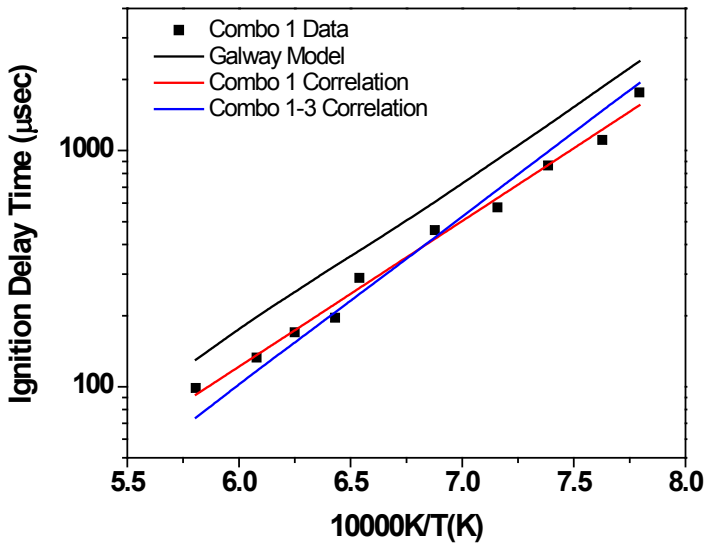

Figure 21 Combination 1 data compared to the Galway model, the correlation for combination 1, and the correlation for combinations 1 through 3.

Figure 22 shows the data from combination 2 experiments compared to the Galway model, the correlation for combination 2, and the correlation for combinations 1 through 3. Again, the correlation for the single combination is seen to lie almost directly on top of the data points, within the 10% error expected for the data. The correlation for combinations 1 through 3 is seen to have moderately good agreement with the data. However, the slope of the line for the multiple-combination correlation at these conditions does not predict the general trend seen in the data. At temperatures outside of the experimental conditions, the multiple-combination correlation would not do a good job of predicting the expected ignition delay times. At lower temperatures, the ignition delay times would be significantly under predicted, and at higher temperatures, the ignition delay times would be significantly over predicted.

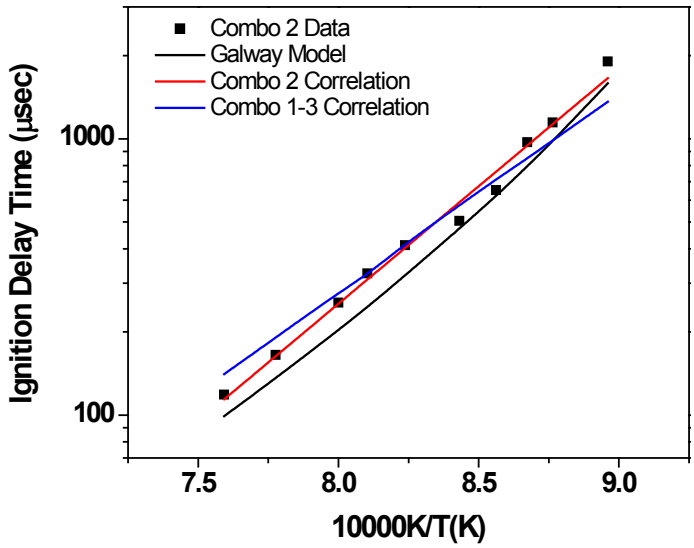

Figure 22 Combination 2 data compared to the Galway model, the correlation for combination 2, and the correlation for combinations 1 through 3.

Data from combination 3 are compared to the Galway model as well as to the correlations for combination 3 and for combinations 1 through 3 in Figure 23. The correlation from combination 3 lies directly on the data points, within the 10% uncertainty level. In general, the correlation from combinations 1 through 3 does a better job of predicting the data than the Galway model. However, the trend of the data is predicted with a significantly different slope so outside of the experimental temperature range, the multiple-combination correlation would predict the ignition delay times incorrectly. Even in the current temperature range, the low-temperature data are noticeably under predicted, while the high temperature data are over predicted.

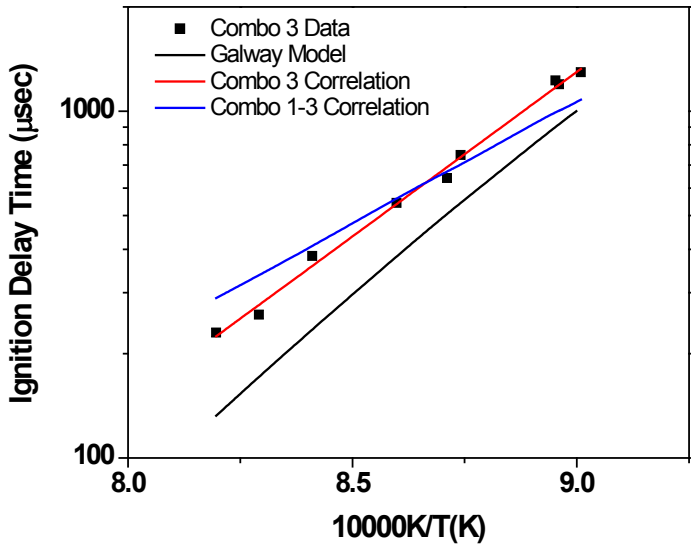

Figure 23 Combination 3 data compared to the Galway model, the correlation for combination 3, and the correlation for combinations 1 through 3.

5.1.2 NG2 Combination Correlations

Individual correlations were developed for combinations 4 through 6 using Eqn. 4. The correlation constants (A) and activation energies (E) for each of these correlations are listed in Table 6. Unlike combinations 1 through 3, the activation energy of the combinations is not seen to increase with the increase of any specific factor (hydrogen, pressure, or equivalence ratio). This shifting activation energy indicates that these combinations are exhibiting a more complex relationship between the three different factors than the methane combinations. This result shows the benefit of using an L9 matrix to capture complex effects of combination variation since more than one value is changing between each experiment.

Table 6 Correlation constants and activation energies found for correlations of combinations 4 through 6 individually.

Combo	A	E (kcal/mol)
4	1.43×10^{-4}	37.0
5	6.61×10^{-4}	35.4
6	1.45×10^{-7}	49.9

In addition, a correlation using Eqn. 5 was developed for these three combinations. This multiple-combination correlation is described in Table 7.

Table 7 Correlation for combinations 4 through 6 using Eqn. 5.

A	x	y	z	E	R^2
4.47×10^{-22}	-0.47	-3.91	1.93	45.9	0.969

The coefficients derived for the correlation of combinations 4 through 6 are significantly closer to unity than the coefficients derived for the initial correlation of combinations 1 through 3. Due to this favorable result, no other correlation attempts were performed.

From the correlation described in Table 7, a few trends in these combinations can be observed. First, the two negative coefficients, *x* and *y*, indicate that the ignition delay time decreases as the concentrations of both NG2 and hydrogen increase. The larger exponent for the hydrogen concentration indicates that small changes in the concentration of hydrogen will affect the ignition delay time more than small changes in

the concentration of NG2. The positive exponent for the oxygen concentration, *z*, indicates that as the concentration of oxygen increases the ignition delay time will also increase. The R^2 value for this correlation is higher than for the previous combination set, which shows that it will likely do a better job of predicting ignition delay times for these combinations, even outside of the experimental conditions tested, although extrapolation of the correlations beyond their stated range of applicability is not recommended.

Again, further information from these correlations can be gained by graphical comparison to the data. In Figure 24 through Figure 26, the data from each combination are compared to the correlations. Additionally, the correlations are compared to the data on a 1 to 1 basis in the appendix

In Figure 24, the data from combination 4 are compared to the Galway model, the correlation for combination 4, and the correlation for combinations 4 through 6. The two correlations essentially lie on top of each other and the data, showing excellent agreement for both correlations. They both predict the experimental data more accurately than the Galway model. Additionally, the slope of the data is also accurately predicted by the correlation for combination 4 and for NG2 correlation for combinations 4 through 6. This level of precision indicates that the both correlations would accurately predict data for this combination, potentially even outside of the temperature range shown in Figure 24.

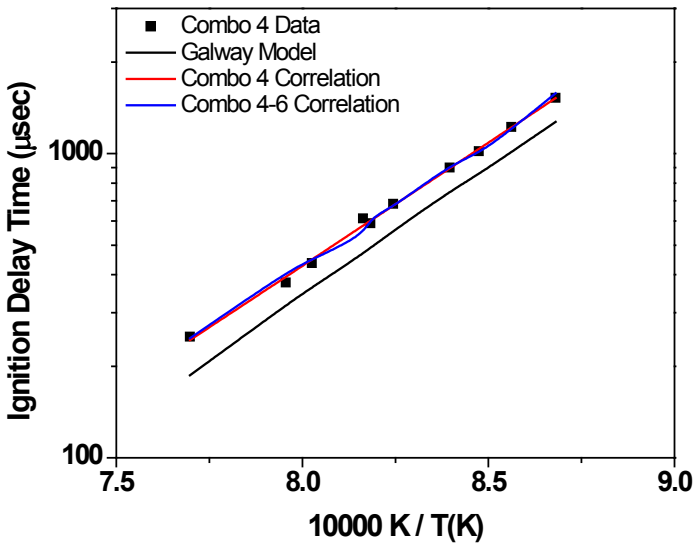

Figure 24 Combination 4 data compared to the Galway model, the correlation for combination 4, and the correlation for combinations 4 through 6.

Experimental data from combination 5 are compared to the Galway model, the correlation for combination 5, and the correlation for combinations 4 through 6 in Figure 25. The correlation designed for only combination 5 is seen to line up directly with the data and can be used to make fairly accurate predictions of this combination. The correlation for combinations 4 through 6 does an adequate job of predicting both the data and the trend of the data. This multiple-combination correlation matches the data within the expected 10% uncertainty, although it does not do quite as good of a job predicting this combination as it did predicting combination 4. However, since the slope of the multiple-combination correlation seems to accurately predict the general trend seen in the data at the extremes of the temperatures in the experimental set, this correlation can

also be used to accurately predict the combination outside of the experimental temperatures.

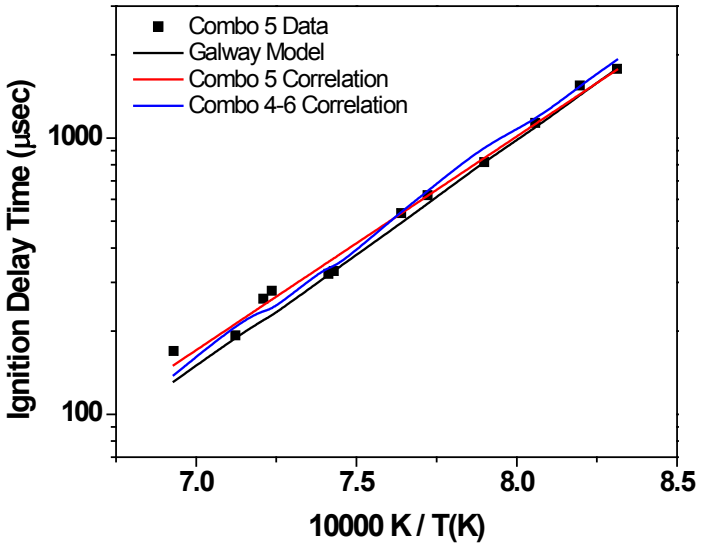

Figure 25 Combination 5 data compared to the Galway model, the correlation for combination 5, and the correlation for combinations 4 through 6.

Figure 26 shows the data from combination 6 compared to the Galway model, the correlation for combination 6, and the correlation for combinations 4 through 6. The correlation for combination 6 appears to predict the combination relatively well. However, the slight change in slope is not captured by this correlation since it is only a linear fit to the data. If one extends the line of the correlation, it appears that it will over predict ignition delay times for higher temperatures and under predict ignition delay times for lower temperatures. The correlation for combinations 4 through 6 also does a fairly good job of predicting the data, but the slope of the multiple-combination correlation is slightly smaller than that of the correlation for only combination 6. Due to

this difference in slope between the two correlations, the multiple-combination correlation will provide better predictions at higher temperatures and worse predictions at lower temperatures than the correlation for combination 6.

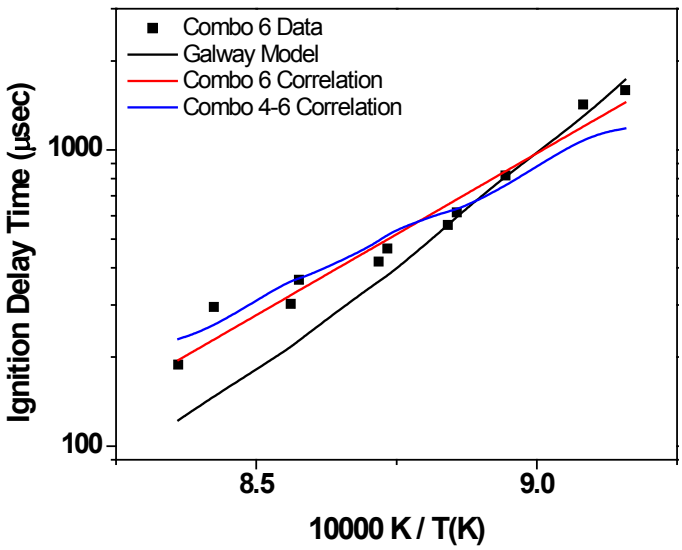

Figure 26 Combination 6 data compared to the Galway model, the correlation for combination 6, and the correlation for combinations 4 through 6.

5.1.3 NG3 Combination Correlations

Similar to the previous sets of combinations, individual correlations were developed for combinations 7 through 9. The correlation coefficients (A) and activation energies (E) for these correlations are listed in Table 8. The activation energies in this case increase with pressure. This trend with pressure indicates that, for these combinations, pressure likely plays a significant role on the reactivity of the combination.

Table 8 Correlation constants and activation energies found for correlations of combinations 7 through 9 individually.

Combo	A	E (kcal/mol)
7	2.69×10^{-4}	36.9
8	3.79×10^{-6}	44.4
9	1.75×10^{-4}	35.0

Additionally, a correlation using the data from all three combinations was developed using Eqn. 5. The coefficients for this correlation are shown in Table 9. The coefficients that were found for the correlation of combinations 7 through 9 were close to or less than unity so no further correlations were attempted.

Table 9 Correlation for combinations 7 through 9 using Eqn. 5.

A	x	y	z	E	R^2
1.04×10^{-7}	0.50	-1.31	0.39	38.7	0.988

The correlation described in Table 9 indicates a few trends in combinations 7 through 9. First, unlike the previous correlation for combinations 4 through 6, the coefficient for the natural gas (NG3), *x*, is positive. This outcome could indicate that the ignition delay times decrease with decreasing NG3 concentration (and increasing H_2 concentration). Similar to the previous multiple-combination correlations, the coefficient for hydrogen concentration, *y*, is negative, while the coefficient for oxygen concentration, *z*, is positive. Therefore, the ignition delay time will decrease with increasing hydrogen

concentration, and the ignition delay time will increase as the oxygen concentration increases. Additionally, the hydrogen concentration has the largest coefficient, so it is likely that hydrogen concentration will play the largest role in determining the ignition delay time of the combinations.

Further information can be gained by graphically comparing the data to these correlations. Figure 27 through Figure 29 show the data from each combination compared to the correlations for that combination. Additionally, 1 to 1 comparisons of the combination correlations to the data are presented in the appendix.

Data from experiments with combination 7 are plotted with the Galway model, the correlation for combination 7, and the correlation for combinations 7 through 9 in Figure 27. Both correlations do an exceptional job of predicting the experimental data. They lie effectively on top of one another and the data. There is a slight difference in the slopes of the two correlations, so at temperatures that are different from the experimental temperatures by about 1000 K, errors in predicting may start to develop. However, the good agreement between the correlations and the data shows that these correlations will be good at predicting ignition delay times within a couple hundred Kelvin of the experimental temperatures.

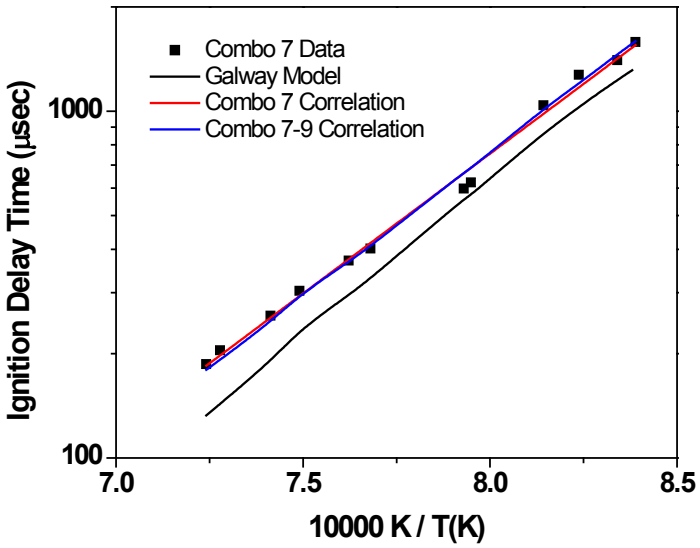

Figure 27 Combination 7 data compared to the Galway model, the correlation for combination 7, and the correlation for combinations 7 through 9.

In Figure 28, the experimental data from combination 8 are plotted with the Galway model as well as with the correlation for combination 8 and the correlation for combinations 7 through 9. The correlation for combination 8 is seen to lie on top of the experimental data, within the 10% expected uncertainty in the data. This correlation will be able to make fairly accurate predictions of this combination, even at temperatures outside of the experimental temperature range. The correlation for combinations 7 through 9 does an inferior job of predicting this combination than was seen for combination 7. In the center of the data set, the correlation predicts the data very well. However, the slope of the correlation is different than that of the data. At higher temperatures, even within the experimental temperatures, the correlation begins to over

predict ignition delay times, and at lower temperatures, the correlation begins to under predict ignition delay times.

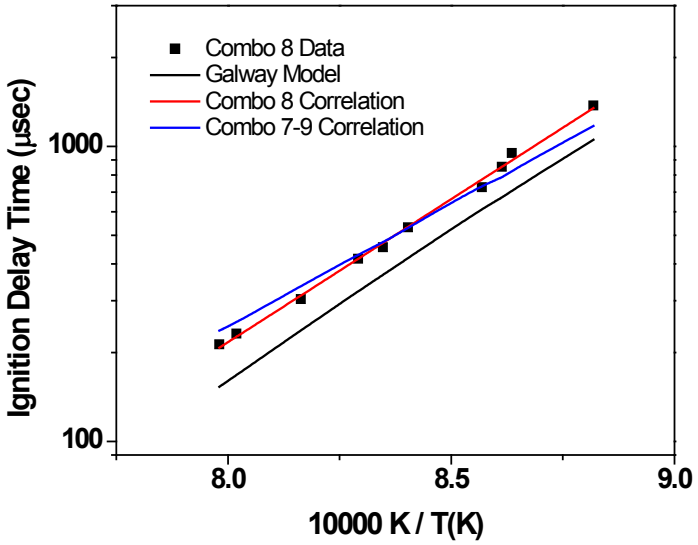

Figure 28 Combination 8 data compared to the Galway model, the correlation for combination 8, and the correlation for combinations 7 through 9.

Figure 29 shows the experimental data for combination 9 compared to the Galway model, the correlation for combination 9, and the correlation for combinations 7 through 9. Both correlations appear to make fairly accurate predictions of the experimental data. The correlation for combination 9 predicts the trend of the data and matches the data points within the expected 10% uncertainty. The multiple-combination correlation also predicts the data mostly within the expected uncertainty. However, the slope of the correlation for combinations 7 through 9 is slightly different than that of the data. Although the data points are well predicted for this temperature range, the multiple-combination correlation will likely not do as well outside of the experimental

temperature range. At lower temperatures, the ignition delay times will be over predicted and at higher temperatures, the ignition delay times will be under predicted.

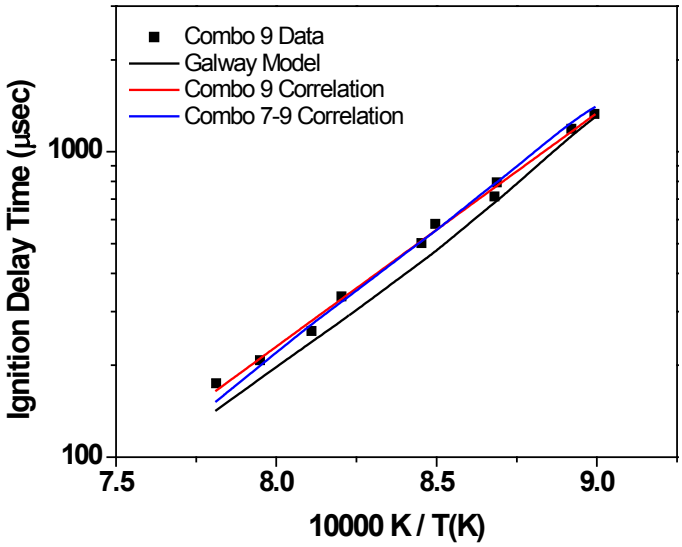

Figure 29 Combination 9 data compared to the Galway model, the correlation for combination 9, and the correlation for combinations 7 through 9.

5.1.4 L9 Matrix Correlations

To develop a correlation that captures all aspects of the L9 matrix and that could be used to predict combinations with any of the natural gases, a few correlation schemes were employed for data from all 9 combinations. First, the original correlation scheme described by Eqn. 5 was employed. However, instead of using the concentration of the natural gas in the combination, only the concentration of methane in each combination was used. This constraint is described by Eqn. 7.

$$\tau_{ign} = A[CH_4]^x[H_2]^y[O_2]^z exp\left(\frac{E}{RT}\right) \quad (7)$$

It should be noted that the methane concentration is different for each combination in the L9 matrix due to all four factors: base natural gas composition, hydrogen fraction of the fuel combination, equivalence ratio, and pressure. The empirically determined coefficients for this correlation are shown in Table 10.

Table 10 First correlation attempt using Eqn. 7 for all 9 combinations in the experimental matrix.

A	x	y	z	E	R^2
$2.63x10^{-5}$	0.68	-0.69	-0.35	31.3	0.834

The conclusions that can be drawn from this correlation are similar to those that were found for the previous correlations. As methane concentration decreases, the ignition delay time will also decrease, and as hydrogen concentration increases, the ignition delay time will decrease. However, the exponent for oxygen, *z*, is negative indicating that as oxygen concentration increases, the ignition delay time will decrease. The R^2 value of the correlation is less than 0.9, indicating that the correlation does not provide acceptable predictions of the experimental data.

A comparison between the predictions from the correlation described by Table 10 and the experimental data is shown in Figure 30. As expected from the low R^2 value, the correlation does not do well at predicting all of the combinations. The combinations that are predicted the worst are combinations 8 and 3. Additionally, all three of the combinations with 60% hydrogen (combinations 2, 5, and 8) are poorly predicted indicating that the

effect of the hydrogen addition is not accurately captured by this correlation. However, combinations 4, 7, and 9 are predicted well with this correlation. This inconsistency amongst the different combinations indicates that the correlation captures some of the effects of the different factors that were changed between the combinations.

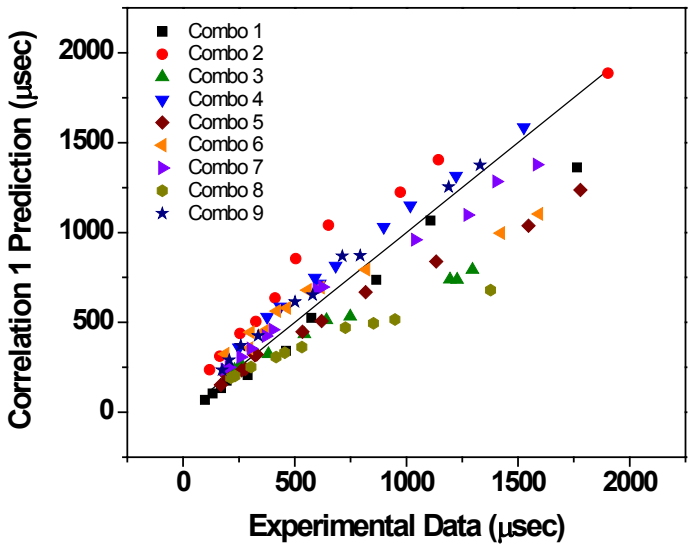

Figure 30 Comparison of the experimental data from all 9 experimental combinations to the predictions from the correlation developed using Eqn. 7. The predicted data are plotted as a function of the real data values with a 1 to 1 line.

Since the R^2 value was low for the correlation described by Table 10, another correlation scheme was attempted. The equation for this correlation is described by Eqn. 8 and incorporates the concentration of argon in each combination.

$$\tau_{ign} = A[CH_4]^x[H_2]^y[O_2]^z[Ar]^w exp\left(\frac{E}{RT}\right) \quad (8)$$

By including the concentration of argon, only the concentration of higher-order hydrocarbons in the base natural gas is not a variable. Again, the concentration of

methane will vary for each combination due to all four factors in the L9 matrix. The values for each coefficient in this correlation are shown in Table 11.

Table 11 Second correlation attempt using Eqn. 8 for all 9 combinations in the experimental matrix.

A	x	y	z	w	E	R^2
$1.65x10^{-11}$	0.19	-1.47	-3.27	4.12	33.1	0.885

The first three exponents, *x*, *y*, and *z*, indicate similar trends as seen with the first correlation; ignition delay time decreases with decreasing methane and increasing hydrogen and oxygen. The effects of hydrogen and oxygen concentrations are seen to be more important, indicated by the larger exponents than seen before. Since the mole fraction of argon in each combination is constant, the effect of the concentration of argon is more of an indication of the effect of changes in the ratio between pressure and temperature. Therefore, the positive exponent for argon concentration indicates that as the ratio between pressure and temperature increases, the ignition delay time increases. It should also be noted that the exponents *z* and *w* are rather far from unity, indicating that an aspect of the correlation is likely over specified.

The ignition delay times predicted by the second correlation are compared to the experimental data in Figure 31. The R^2 value for this correlation was an improvement from the first correlation, although still not above the desired value of at least 0.9. This slightly better coefficient of multiple determination can be seen in the figure as the

experimental data are predicted a little better in most cases than in Figure 30. The same combinations are still noticeably under predicted (combinations 5, 6, and 8), indicating a similar issue with the prediction of the effect of hydrogen on the combinations. Combination 2 is under predicted by this correlation at higher ignition delay times, the opposite of what was seen with the previous correlation. Additionally, combinations 4 and 9 are noticeably over predicted. The prediction of combination 6 is similar between the two correlations, and the second correlation does a reasonable job of predicting combinations 1 and 7.

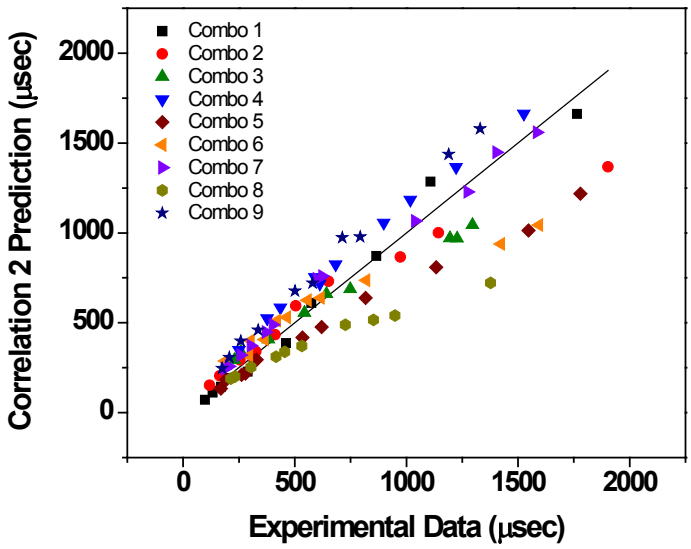

Figure 31 Comparison of the experimental data from all 9 experimental combinations to the predictions from the correlation developed using Eqn. 8. The predicted data are plotted as a function of the real data values with a 1 to 1 line.

Due to the large exponents for argon and oxygen concentration in the previous correlation, one further correlation was attempted for the full set of experimental data.

This correlation is described by Eqn. 9 and attempted to incorporate the concentration of the entire natural gas, instead of only the methane component.

$$\tau_{ign} = A[NG]^x[H_2]^y[O_2]^z[Ar]^w\left[x_{Fuel\_CH_4}\right]^v exp\left(\frac{E}{RT}\right) \quad (9)$$

In the correlation described by Eqn. 9, *[NG]* is the concentration of the entire natural gas in the experiment, and $x_{Fuel\_CH_4}$ is the mole fraction of methane in the natural gas. Using this correlation, the exponents were found and are described in Table 12.

Table 12 Third correlation attempt using Eqn. 9 for all 9 combinations in the experimental matrix.

A	x	y	z	w	v	E	R^2
$8.52x10^{-12}$	0.15	-1.50	-3.36	4.30	0.32	33.2	0.887

The exponents *y*, *z*, and *w* are almost the same as what found for the previous correlation indicating that this correlation captures similar trends. However, they are even further from unity than for the previous correlation. The exponent for the concentration of the natural gas, *x*, is extremely small, indicating that the effect of the natural gas in the combination is almost negligible. The positive exponent *v* indicates that as methane content in the natural gas increases (and the higher-order hydrocarbon content decreases) the ignition delay time increases, which was expected.

A comparison between the ignition delay time predictions of the third correlation and the experimental data is shown in Figure 32. This comparison is extremely similar to that

shown for the second correlation. This similarity was expected since the exponents for the two correlations are similar and the R^2 values are also similar.

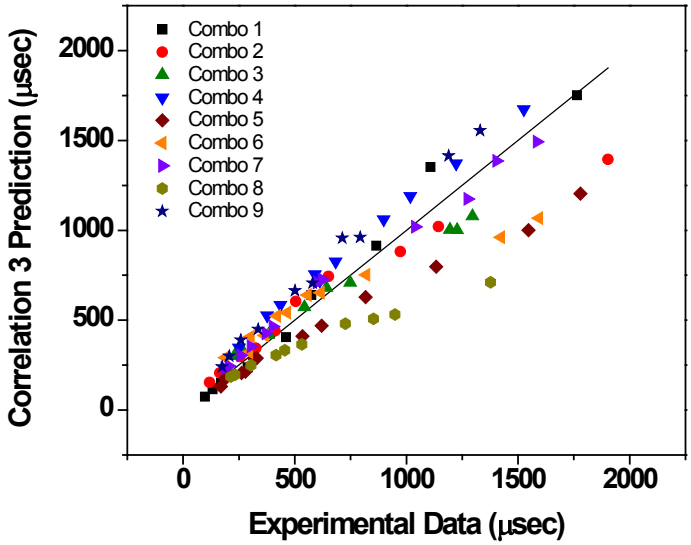

Figure 32 Comparison of the experimental data from all 9 experimental combinations to the predictions from the correlation developed using Eqn. 9. The predicted data are plotted as a function of the real data values with a 1 to 1 line.

All of the correlations for the entire experimental data set were seen to do a poor job of predicting the data from all 9 combinations. This result is likely due to nonlinear effects introduced by the addition of hydrogen to the hydrocarbon fuels combined with effects from changing the natural gas composition, pressure, and equivalence ratio. However, it is beyond the scope of this thesis to develop a more-accurate correlation including these nonlinear effects. The best correlation from the brief exploration described in this section would be the second correlation, described by Eqn. 8 and Table 11. Although the R^2 value of this correlation is slightly lower than that for the third correlation, the exponents are closer to unity. Using a correlation with smaller exponents allows for better

prediction of combinations outside of the 9 combinations studied herein. However, due to the still large exponents and poor R^2 value of this correlation, care should be taken when predicting ignition delay times with this correlation, especially outside of the experimental conditions studied within this thesis.

5.2 L9 Matrix Factor Sensitivity

A factor sensitivity was performed on the results from the L9 matrix to determine which aspect of the combinations plays the largest role in reactivity. By utilizing the L9 Matrix in this manner, fewer experiments can be performed to gain the same information. The four factors considered for the sensitivity analysis were C_{2+} (hydrocarbons higher than methane) content of the natural gas, hydrogen percentage of the fuel, equivalence ratio, and pressure.

The correlations for each individual combination (described in Table 3, Table 6, and Table 8) were used to predict ignition delay times for each combination at different temperatures. These correlations were used because it was found that for every combination, the single combination correlations very accurately described the data, usually without the risk of over or under prediction of the ignition delay time outside of the experimental temperature range.

Four temperatures were chosen close to the experimental temperatures used throughout the matrix: 1100 K, 1150 K, 1200 K, and 1250 K. After ignition delay times were found

for each combination at each temperature, an average of the ignition delay times of combinations with a factor at a certain level were taken at each temperature. For example, an average of ignition delay times at 1100 K was taken for each: combinations containing CH_4 (C_{2+} level 1), combinations containing NG2 (C_{2+} level 2), and combinations containing NG3 (C_{2+} level 3). Then, the maximum difference between averages was taken to be the sensitivity of that factor, at that temperature. Continuing the same example, differences were found between the CH_4 average and the NG2 average at 1100 K, between the NG2 average and the NG3 average at 1100 K, and between the NG3 average and the CH_4 average at 1100 K. The maximum of these three differences was taken to be the sensitivity of C_{2+} content of the natural gas on the ignition delay time at 1100 K. This procedure was repeated to find the factor sensitivities of each factor at each temperature. Finally, at each temperature, all four factor sensitivities were normalized to the largest sensitivity. The normalization of the factor sensitivities allowed for comparison at different temperatures.

The factor sensitivity analysis for predicted ignition delay times of the full L9 matrix is shown in Figure 33. This analysis indicates that the hydrogen content of the fuel mixture is the most important factor. It was expected that hydrogen would play a significant role in determining the reactivity of these combinations because hydrogen reactivity is known to be significantly higher than for hydrocarbons at the same conditions.

The second most important factor in the matrix studied was pressure. The effect of pressure is seen to increase as temperature increases and is close to as important as hydrogen content at the highest temperature. This level of importance was expected since, for all of the base components of the combinations, variations in pressure have been shown to greatly affect the ignition delay time.

Equivalence ratio was a moderately significant factor in the matrix studied. Although the effect was not negligible, equivalence ratio did not affect the reactivity of the combinations as strongly as hydrogen content or pressure. The effect of equivalence ratio at lean conditions is due to the increased importance of oxygen for chain branching kinetics. However, this effect is also closely linked to the effects of pressure and composition of the fuel mixture.

Finally, the C_{2+} fraction of natural gas was seen to have the smallest effect on the ignition delay times. However, the effect was not negligible. This smaller effect was expected since the reactivities of the different natural gases used in this matrix were relatively similar when compared to the reactivity of hydrogen. However, the effect of C_{2+} content of the natural gas increased relative to the effects of the other factors with temperature. This result is likely due to the fact that ignition delay times of methane decrease as temperature increases at a much slower rate than NG2 or NG3 ignition delay times (Bourque et al., 2010).

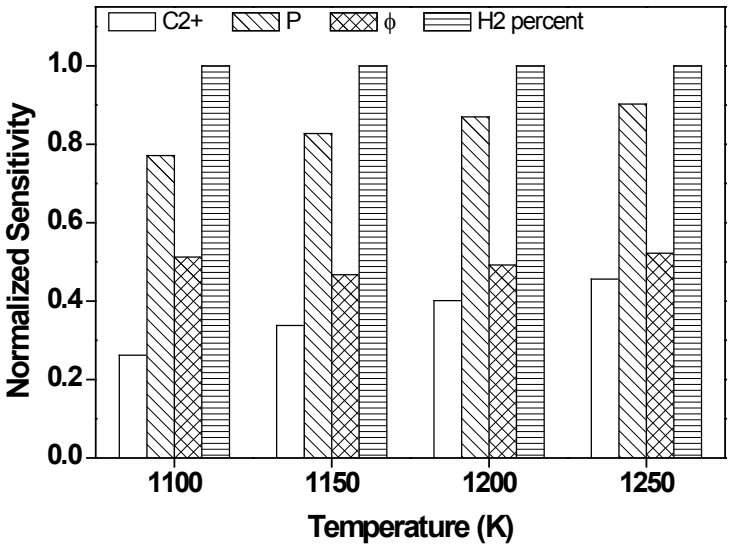

Figure 33 Factor sensitivity of the L9 matrix at four temperatures (1100 K, 1150 K, 1200 K, and 1250 K) for the four factors of the matrix (C_{2+} content of the natural gas, H_2 content of the fuel, equivalence ratio, and pressure).

5.3 Full Matrix Calculations

To determine if any effects of the factors that were varied in the experiments were missed by using the reduced L9 matrix, calculations using the Galway mechanism and CHEMKIN were performed for the full factorial, or full, matrix. The full matrix is defined as every possible combination from the factors varied in the L9 matrix. This exercise results in 3^4 (81) different combinations, or 27 combinations for each natural gas, which are detailed in Table 13. Ignition delay times were calculated for each combination at four or more different temperatures. In the end, the full matrix consisted of a total of 544 calculations. One main purpose of the calculations in this section was to

demonstrate the utility of employing reduced matrices in lieu of full matrices when studying the ignition (or other kinetic) behavior of fuel blends.

Similar to the correlations from the L9 matrix, the discussion of the full matrix is split into combinations containing methane, NG2, and NG3. Using the full matrix calculations, a separate L9 matrix was developed for each individual natural gas set. These L9 matrices were the same as the L9 matrix originally described except the natural gas was kept constant. Described in the following subsections are correlations developed from the full matrix for each natural gas set and correlations developed from the L9 matrix for each natural gas set. These correlations are compared to the full matrix data as well as the L9 matrix data to determine if the L9 matrices of each natural gas define the same trends seen in the full matrix of each natural gas. Additionally, a factor sensitivity analysis was performed for each L9 matrix to predict how the effect of each factor would change as the C_{2+} content of the base natural gas increases.

Table 13 Full matrix calculations performed for each natural gas (NG), methane, NG2, and NG3.

Combo	Fuel	$\%H_2$	ϕ	P (atm)
1	NG	30	0.3	1
2	NG	30	0.3	10
3	NG	30	0.3	30
4	NG	30	0.5	1
5	NG	30	0.5	10
6	NG	30	0.5	30
7	NG	30	1	1
8	NG	30	1	10
9	NG	30	1	30
10	NG	60	0.3	1
11	NG	60	0.3	10
12	NG	60	0.3	30
13	NG	60	0.5	1
14	NG	60	0.5	10
15	NG	60	0.5	30
16	NG	60	1	1
17	NG	60	1	10
18	NG	60	1	30
19	NG	90	0.3	1
20	NG	90	0.3	10
21	NG	90	0.3	30
22	NG	90	0.5	1
23	NG	90	0.5	10
24	NG	90	0.5	30
25	NG	90	1	1
26	NG	90	1	10
27	NG	90	1	30

5.3.1 Methane Calculations

The 27 possible combinations containing methane were calculated at four or more temperatures each. Using these calculations, a full matrix correlation was constructed using Eqn. 5. The coefficients that were found for this matrix are shown in Table 14. An L9 matrix was developed for methane mixtures and is described in Table 15. The correlation from this L9 matrix, also developed using Eqn. 5, is described by the coefficients listed in Table 16.

Table 14 Correlation coefficients for a correlation developed from the full matrix calculations for methane.

A	x	y	z	E	R^2
4.77×10^{-6}	1.44	-1.14	-0.82	31.2	0.931

Table 15 L9 Matrix for methane.

Combo	Fuel	$\%H_2$	ϕ	P (atm)
1	CH_4	30	0.3	1
2	CH_4	60	0.5	10
3	CH_4	80	1	30
4	CH_4	30	0.5	30
5	CH_4	60	1	1
6	CH_4	80	0.3	10
7	CH_4	30	1	10
8	CH_4	60	0.3	30
9	CH_4	80	0.5	1

Table 16 Correlation coefficients for a correlation developed from the L9 matrix for methane.

A	x	y	z	E	R^2
$3.44x10^{-6}$	1.52	-1.17	-0.92	31.1	0.941

An examination of the coefficients listed in Table 14 and Table 16 show relatively good agreement. This favorable result indicates that the trends within the entire matrix of methane combinations can be captured by using fewer combinations. For both correlations, the exponential coefficient of methane, *x*, is positive (1.44 and 1.52). This result shows that, as expected, the ignition delay time increases as the concentration of methane in the fuel mixture increases (and the concentration of hydrogen decreases). Conversely, the exponential coefficients of H_2 and O_2, *y* and *z*, respectively, are negative (-1.14 and -1.17; and -0.82 and -0.92). In the hydrogen case, this result indicates that as the H_2 content of the fuel mixture increases, the ignition delay time will decrease. This trend was expected since it is what was found from the original L9 matrix and because the ignition delay times of pure hydrogen are shorter than the ignition delay times of pure methane. The negative exponent for oxygen concentration indicates that as the concentration of oxygen in the mixture decreases the ignition delay time will increase. Additionally, the activation energies (*E*) found for these combinations (about 31 kcal/mol for both matrices) is relatively close to that found for the experimental methane combinations (37 kcal/mol, on average, Table 3). This consistency indicates that the combinations used in the full matrix came close to correctly estimating the activation energies for methane combinations from the experiments.

In Figure 34 and Figure 35, comparisons between the two correlations described above are made to the methane L9 matrix data. Figure 34 shows the comparison between the methane L9 data and predictions for the same data made using the full matrix correlation. The points that are over predicted in this graph are from the combination with 80% hydrogen in the fuel mixture at an equivalence ratio of 0.5 and a pressure of 1 atm. The ignition delay times that are significantly under predicted are from the combination with 60% hydrogen in the fuel mixture with a phi of 0.5 and a pressure of 30 atm. Similarly, in Figure 35 the data from the methane L9 matrix is compared to the predictions from the L9 matrix correlation for methane. The comparison appears to be almost the same as that shown for the full matrix predictions. This agreement between the two correlations indicates that the correlation from only the L9 matrix captures the most significant aspects of the full-matrix correlation.

To further prove that the methane L9 matrix correlation captures the same features as the full-matrix correlation, all of the data from the methane full matrix calculations were compared to both correlations. The full matrix correlation is compared to the data in Figure 36, and the methane L9 matrix correlation is compared to the data in Figure 37. The similarity between the two figures shows that the L9 matrix captures all of the aspects of changing the combinations and conditions that the full matrix does. Both correlations do a poor job predicting long ignition delay times, but they produce similar results. In general, the most under predicted ignition delay times are found for combinations that are 80% hydrogen, while the most over predicted ignition delay times

are found for combinations that are 30% hydrogen. This dependence on H_2 implies that hydrogen addition has a nonlinear effect on the ignition delay times of methane mixtures that is not captured by correlations of the form of Eqn. 5. While further analysis could be performed to determine an appropriate correlation scheme, as was done for syngas mixtures (Donato and Petersen, 2008), it is beyond the scope of the present work.

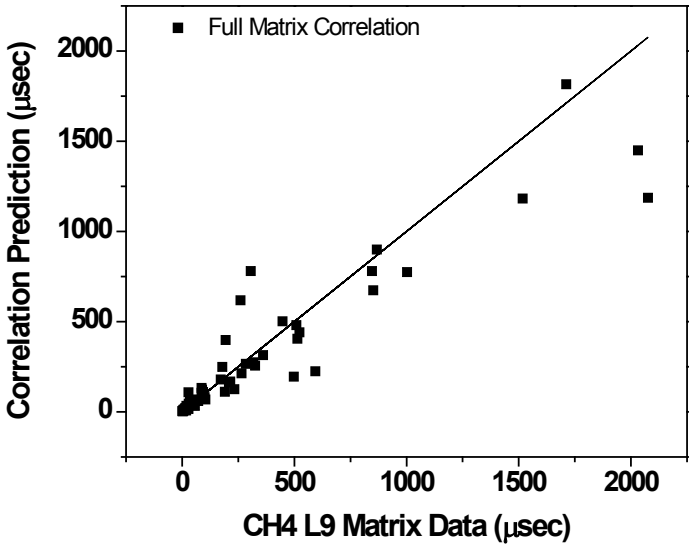

Figure 34 Comparison of the data used in the methane L9 matrix to the full matrix correlation. The predicted data are plotted as a function of the real data values with a 1 to 1 line.

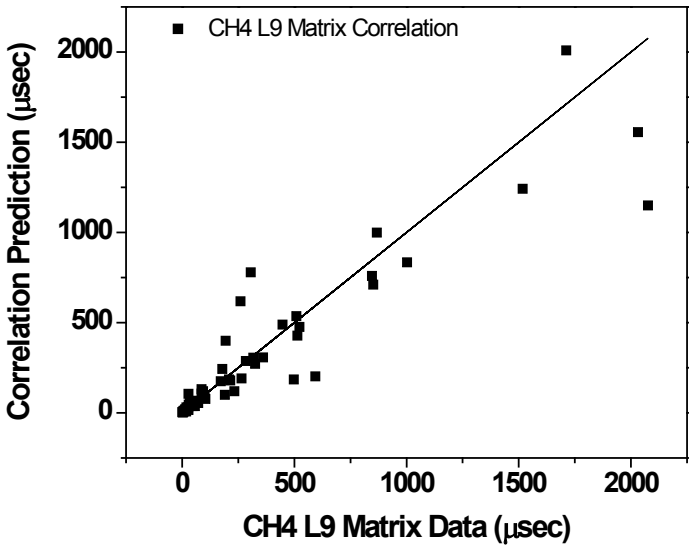

Figure 35 Comparison of the data used in the methane L9 matrix to the methane L9 matrix correlation. The predicted data are plotted as a function of the real data values with a 1 to 1 line.

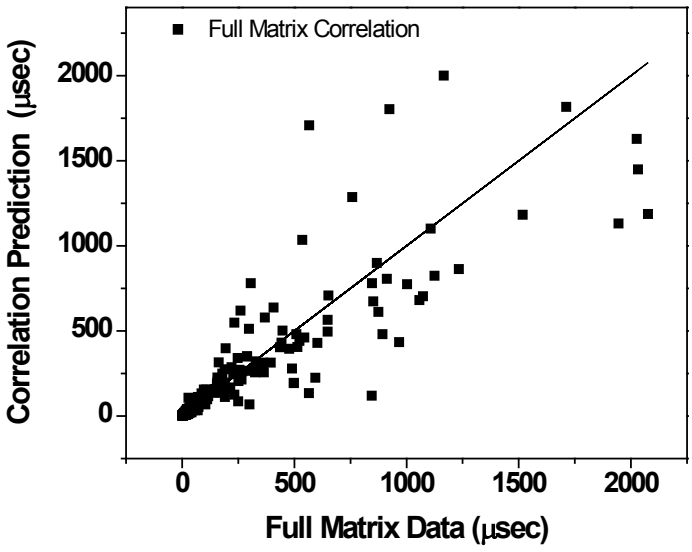

Figure 36 Comparison of the data used in the full matrix to the methane full matrix correlation. The predicted data are plotted as a function of the real data values with a 1 to 1 line.

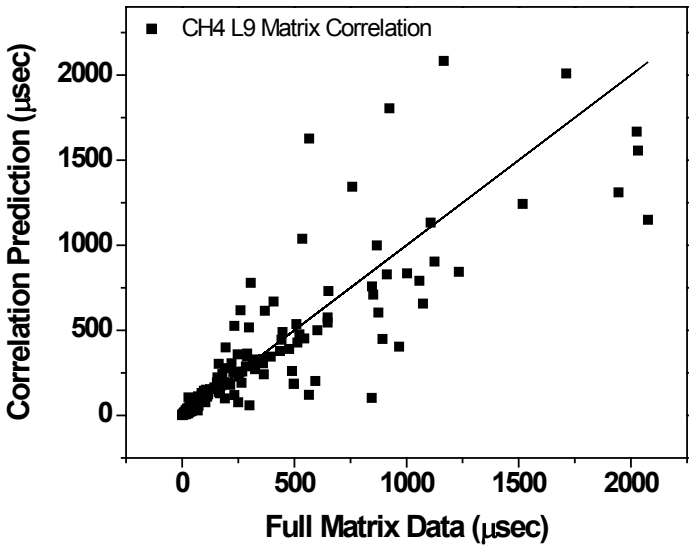

Figure 37 Comparison of the data used in the full matrix to the methane L9 matrix correlation. The predicted data are plotted as a function of the real data values with a 1 to 1 line.

A final step of the analysis of the methane calculations from the methane L9 matrix was to perform a factor sensitivity analysis for the matrix. Since the correlation from the L9 matrix and the correlation from the full matrix were proven to provide similar predictions, only the nine combinations in the L9 matrix were used. Similar to the previous factor sensitivity, correlations for each individual combination, listed in Table 17, were used to predict ignition delay times at a few temperatures.

Table 17 Correlations for individual combinations of the methane L9 matrix.

Combo	A	E (kcal/mol)
1	1.91×10^{-2}	29.8
2	8.62×10^{-4}	31.0
3	3.87×10^{-5}	36.6
4	3.24×10^{-5}	42.6
5	4.26×10^{-2}	24.9
6	8.79×10^{-6}	27.3
7	1.16×10^{-3}	36.1
8	1.59×10^{-5}	41.0
9	8.39×10^{-2}	18.5

The factor sensitivity, described in detail previously, was performed at four temperatures (1100 K, 1150 K, 1200 K, and 1250 K). The resulting factor sensitivities were normalized and are shown in Figure 38. It is seen from this figure that hydrogen content of the fuel mixture far outweighs any other factor. In fact, the hydrogen factor sensitivity is more than double the sensitivity of any other factor at every temperature. This increase in sensitivity to the hydrogen content of the fuel mixture from the experimental L9 matrix is likely due to the fact that methane has a significantly lower reactivity than pure hydrogen and the other two natural gases used in the study. Adding hydrogen to pure methane will almost always dramatically increase the reactivity of the mixture, despite the pressure or equivalence ratio. The other two factors, pressure and equivalence ratio, are seen to change order of importance as temperature increases. At lower temperatures, equivalence ratio is more important than pressure. At higher temperatures, the pressure of the mixture is more important than the equivalence ratio.

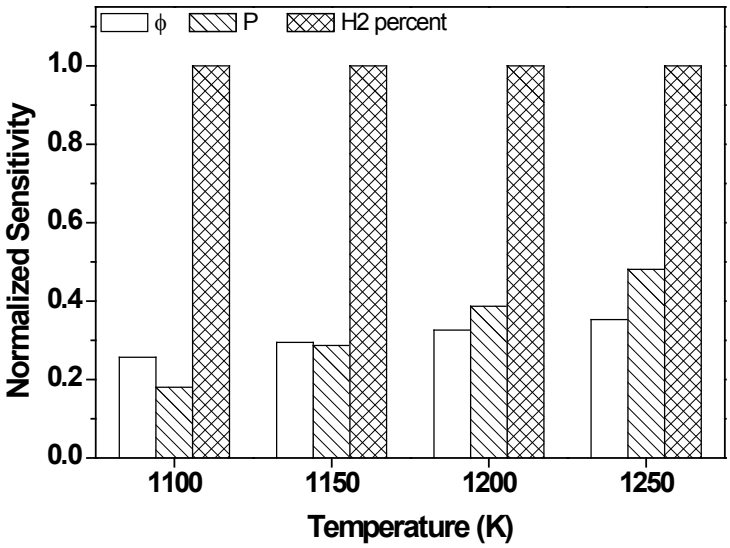

Figure 38 Factor sensitivity of the methane L9 matrix at four temperatures (1100 K, 1150 K, 1200 K, and 1250 K) for the three factors of the matrix (H_2 content of the fuel, equivalence ratio, and pressure).

5.3.2 NG2 Calculations

Similar to the methane calculations, full matrix calculations were performed for NG2 combinations. The same three factors were varied: hydrogen content of the fuel mixture, equivalence ratio, and pressure. Using the 27 combinations from the full matrix calculation, a correlation was developed, described by Table 18. Nine combinations from the 27 were used to develop an L9 matrix from the calculations, described by Table 19. A correlation was derived from these 9 combinations and is described by Table 20.

Table 18 Correlation coefficients for a correlation developed from the full matrix calculations for NG2.

A	x	y	z	E	R^2
$4.71x10^{-7}$	1.09	-0.68	-0.83	39.8	0.974

Table 19 L9 Matrix for NG2.

Combo	Fuel	$\%H_2$	ϕ	P (atm)
1	NG2	30	0.3	1
2	NG2	60	0.5	10
3	NG2	80	1	30
4	NG2	30	0.5	30
5	NG2	60	1	1
6	NG2	80	0.3	10
7	NG2	30	1	10
8	NG2	60	0.3	30
9	NG2	80	0.5	1

Table 20 Correlation coefficients for a correlation developed from the L9 matrix for NG2.

A	x	y	z	E	R^2
$2.90x10^{-7}$	1.15	-0.67	-0.94	40.5	0.980

Similar to what was seen with the methane correlations, the coefficients for the two correlations of NG2 calculations are very similar. This similarity again indicates that the trends seen in all of the possible combinations of the full matrix can be predicted with the same accuracy by only using the L9 matrix. The NG2 exponent, *x*, is positive so, similar to methane, the ignition delay time increases as NG2 content increases. It is

significant that the value for x in Table 20 (1.15) is lower than the value for x in Table 16 (1.52). This comparison shows that methane content has more effect on the combination reactivity than NG2, or, in other words, decreasing the methane concentration by adding hydrogen to the fuel mixture will have a greater effect than decreasing the NG2 concentration. This result was expected since the reactivity of methane is lower than NG2. The coefficients for hydrogen and oxygen concentration were again found to be negative; however, the exponent of the oxygen concentration, z, is larger than the exponent for the hydrogen concentration, y, the opposite of what was found for the methane correlations. The opposite trend indicates a shift in the impact of hydrogen concentration to being almost equal to, if not less than, that of equivalence ratio and pressure.

In Figure 39 and Figure 40, comparisons are made between the two correlations presented above and the data used to make the L9 matrix. Figure 39 shows the comparison between the L9 matrix data for NG2 compared to the predictions made by the full matrix correlation at the same conditions. The NG2 full matrix correlation appears to do a better job at predicting the data than the full matrix correlation for methane. Similar to the methane combinations, the most over predicted points are for combinations with 80% hydrogen in the fuel mixture at an equivalence ratio of 0.5 and a pressure of 1 atm. There are two combinations that are under predicted: 60% hydrogen with an equivalence ratio of 1 at a pressure of 1 and 60% hydrogen with an equivalence ratio of 0.3 and a pressure of 30 atm. In Figure 40, the NG2 L9 matrix data are compared

to predictions from the NG2 L9 matrix. The plot looks similar to the previous figure, and the same combinations are under and over predicted as observed with the full matrix correlation. This result again indicates that the correlation from the NG2 L9 matrix manages to capture the most significant aspects of the full matrix correlation, while missing the same few aspects.

The complete set of data used to compile the full matrix correlation for NG2 was compared to predictions from both the full matrix correlation, shown in Figure 41, and the NG2 L9 matrix correlation, shown in Figure 42. The similarity between the two figures indicates that the L9 matrix correlation is able to capture the same predictions as the full matrix correlation, even without using the data from the additional combinations. Additionally, both correlations do a better job of predicting the ignition delay times of NG2 combinations than the previous correlations did for methane combinations. The most under predicted ignition delay times are generally found for combinations with 30% hydrogen, while the most over predicted ignition delay times are generally found for combinations with 80% hydrogen. This trend is again likely due to the nonlinear effect of hydrogen addition to a hydrocarbon mixture. Although it is beyond the scope of this work, further analysis could be performed to find additional correlations that model this effect, similar to Donato and Petersen (2008).

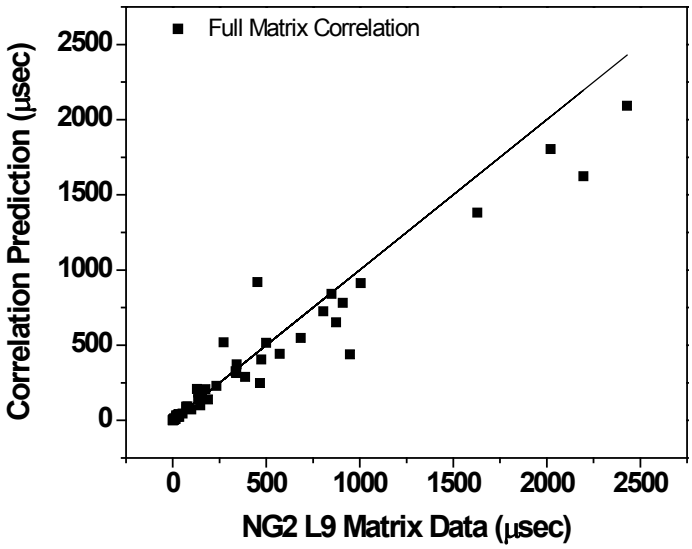

Figure 39 Comparison of the data used in the NG2 L9 matrix to the full matrix correlation. The predicted data are plotted as a function of the real data values with a 1 to 1 line.

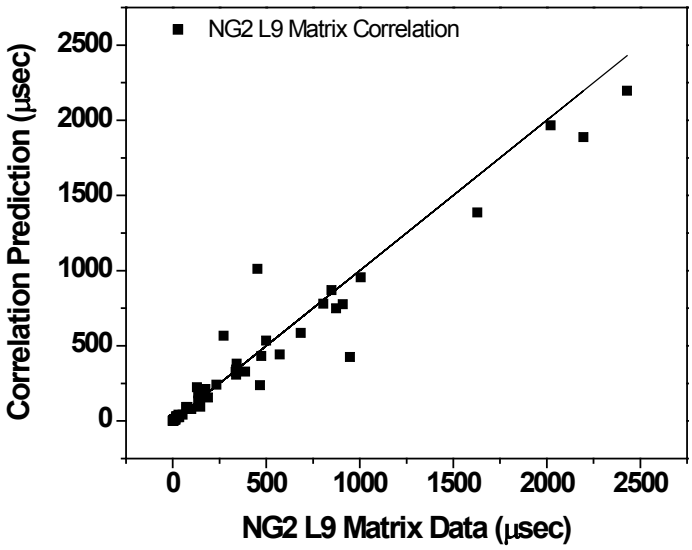

Figure 40 Comparison of the data used in the NG2 L9 matrix to the NG2 L9 matrix correlation. The predicted data are plotted as a function of the real data values with a 1 to 1 line.

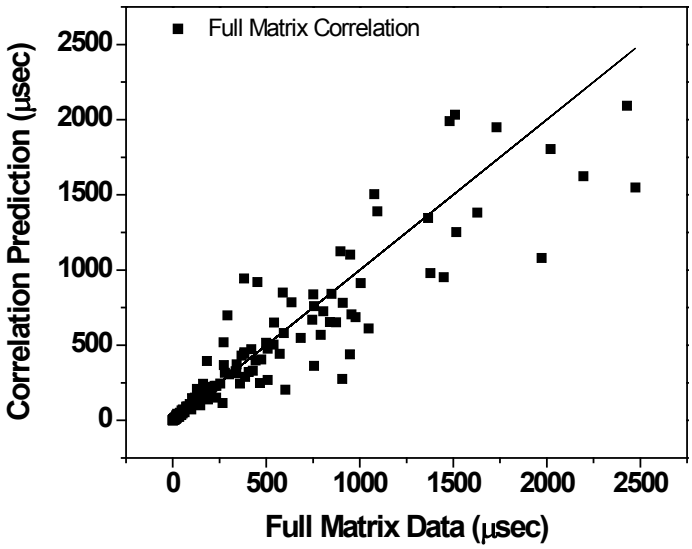

Figure 41 Comparison of the data used in the full matrix to the NG2 full matrix correlation. The predicted data are plotted as a function of the real data values with a 1 to 1 line.

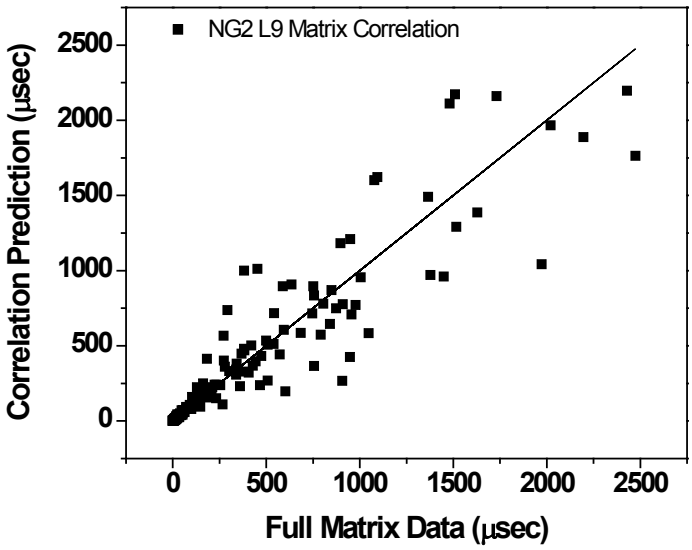

Figure 42 Comparison of the data used in the full matrix to the NG2 L9 matrix correlation. The predicted data are plotted as a function of the real data values with a 1 to 1 line.

The final step in the analysis of the NG2 L9 matrix was a factor sensitivity analysis for the matrix. The correlation from the NG2 L9 matrix was found to be almost identical to the correlation using the full matrix, so only the 9 combinations in the NG2 L9 matrix were used. Correlations found for each individual combination of the NG2 L9 matrix, listed in Table 21, were used to predict the ignition delay times of each combination at a few different temperatures.

Table 21 Correlations for individual combinations of the NG2 L9 matrix.

Combo	A	E (kcal/mol)
1	1.02×10^{-4}	39.9
2	2.62×10^{-5}	39.5
3	7.77×10^{-6}	40.8
4	1.02×10^{-5}	43.2
5	3.53×10^{-4}	36.8
6	1.74×10^{-5}	38.0
7	5.68×10^{-5}	41.1
8	2.23×10^{-6}	45.2
9	8.02×10^{-4}	30.5

A factor sensitivity was applied to the matrix as described earlier. Ignition delay times were found at four temperatures (1100 K, 1150 K, 1200 K, and 1250 K), and the resulting factor sensitivities were normalized for each temperature. Figure 43 shows that the hydrogen content of the fuel mixture is again the main factor in determining the ignition delay times of the combinations. However, the effect of hydrogen is less important compared to the other factors than it was for the methane L9 matrix, especially

at higher temperatures. Hydrogen likely plays less of a role in the reactivity of the NG2 combinations because the reactivity of NG2 is closer to the reactivity of pure hydrogen. The correlations for NG2 already alluded to this reduced sensitivity to hydrogen, but the factor sensitivity also demonstrates that the relative importance of hydrogen decreases with temperature. The effects of pressure and equivalence ratio are shown to have a greater effect relative to the hydrogen effect than they had on the methane combinations.

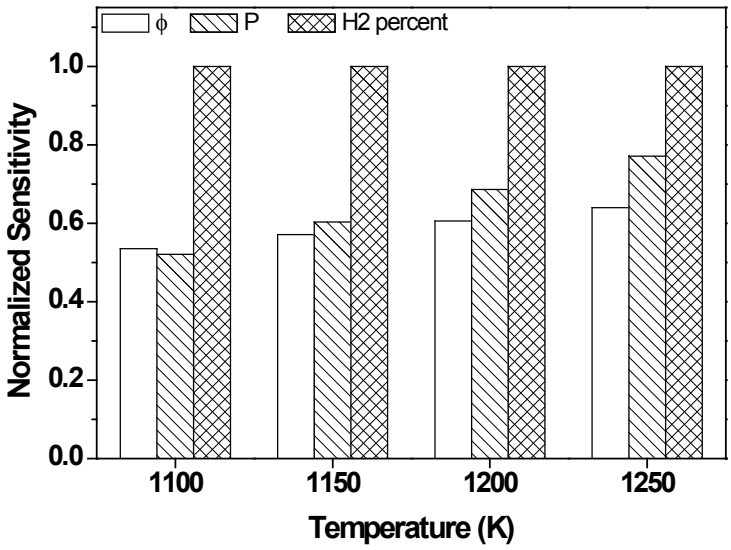

Figure 43 Factor sensitivity of the NG2 L9 matrix at four temperatures (1100 K, 1150 K, 1200 K, and 1250 K) for the three factors of the matrix (H_2 content of the fuel, equivalence ratio, and pressure).

5.3.3 NG3 Calculations

Full matrix and L9 calculations were also performed for NG3 combinations. Again, hydrogen content of the fuel mixture, equivalence ratio, and pressure were varied between the different combinations. From the full matrix calculations, including all 27 possible combinations, a correlation was developed, shown in Table 22. From the 27

combinations used in the full matrix calculations, nine combinations were used to develop an NG3 L9 matrix, described in Table 23. Using the calculations of ignition delay times for these nine combinations, a correlation was developed, described by Table 24.

Table 22 Correlation coefficients for a correlation developed from the full matrix calculations for NG3.

A	x	y	z	E	R^2
$1.08x10^{-7}$	0.95	-0.50	-0.93	42.0	0.984

Table 23 L9 Matrix for NG3.

Combo	Fuel	$\%H_2$	ϕ	P (atm)
1	NG3	30	0.3	1
2	NG3	60	0.5	10
3	NG3	80	1	30
4	NG3	30	0.5	30
5	NG3	60	1	1
6	NG3	80	0.3	10
7	NG3	30	1	10
8	NG3	60	0.3	30
9	NG3	80	0.5	1

Table 24 Correlation coefficients for a correlation developed from the L9 matrix for NG3.

A	x	y	z	E	R^2
$1.30x10^{-7}$	1.02	-0.49	-1.01	41.9	0.985

There is again excellent agreement between coefficients found for the full matrix correlation (Table 22) and the L9 matrix correlation (Table 24). The values for the individual exponents as well as the values for *A* and *E* are extremely similar. Therefore, the trends seen in all 27 combinations can be predicted with the same accuracy using a correlation with only 9 combinations. The R^2 value for both correlations is greater than 0.98, which indicates that both correlations should also correspond quite will with the data. As seen with the NG2 combinations, the exponent for the natural gas, *x*, is positive while the exponents for hydrogen and oxygen concentrations, *y* and *z*, respectively, are negative. Therefore, the ignition delay time will increase when the concentration of NG3 increases compared to hydrogen in the fuel mixture. Also, the ignition delay time will increase when hydrogen or oxygen concentration decreases in the mixture. Since the hydrogen exponent is even smaller than the oxygen exponent than for the NG2 combinations, the impact of hydrogen concentration will not be as significant as seen before.

In Figure 44 and Figure 45 comparisons are made between the correlations for the full matrix and the L9 matrix to the data used for the L9 matrix. A comparison between the NG3 L9 matrix data to the predictions made by the full matrix correlation at the same conditions is shown in Figure 44. For the most part, the full matrix correlation appears to do an accurate job of predicting the L9 matrix data, which was expected due to the R^2 value close to unity for this correlation. Similar to the correlation studies for methane and NG2 combinations, the most over predicted ignition delay times are found for the

combination that is 80% hydrogen at an equivalence ratio of 0.5 and at a pressure of 1 atm. Also, as seen with the NG2 correlations, the most under predicted combinations are 60% hydrogen at an equivalence ratio of 1 and a pressure of 1 atm; and 60% hydrogen with an equivalence ratio of 0.3 and a pressure of 30 atm. A similar comparison between the L9 matrix correlation and the L9 matrix data is shown in Figure 45. As expected from the similarity in the two correlations, the figures look almost identical. This similarity again illustrates that the L9 matrix captures the features that are predicted by using the full matrix for correlations.

The complete set of data used for the full matrix correlation of NG3 is compared to predictions from the full matrix correlation in Figure 46 and to predictions from the L9 matrix correlation in Figure 47. The similarity between the two figures again illustrates the effectiveness of using the L9 matrix to capture the trends seen in the full matrix. Generally, as seen with the previous correlations, the 30% hydrogen combinations tend to be the most under predicted, while the 80% hydrogen combinations tend to be the most over predicted. This behavior is likely due to the fact that addition of hydrogen to the combinations does not have a linear relationship with ignition delay time. Since Eqn. 5 is a linear correlation (on a log plot), the correlations presented are likely missing the true effect of hydrogen addition to these combinations. However, it is beyond the scope of this work to further develop the correlations, similar to what was performed by Donato and Petersen (2008).

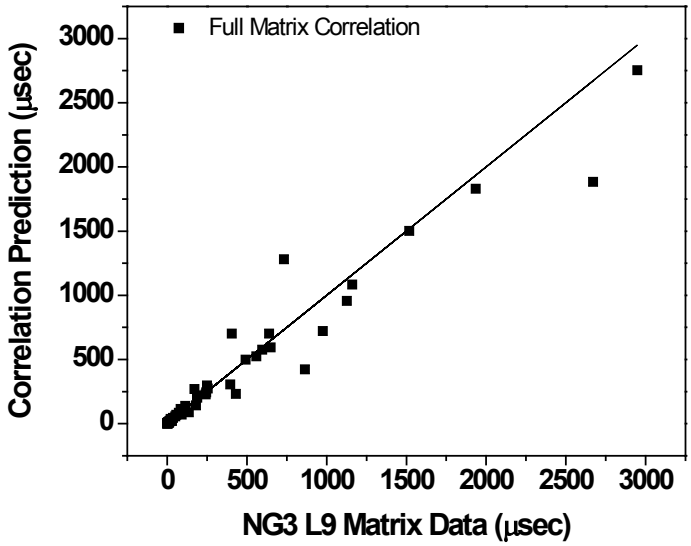

Figure 44 Comparison of the data used in the NG3 L9 matrix to the full matrix correlation. The predicted data are plotted as a function of the real data values with a 1 to 1 line.

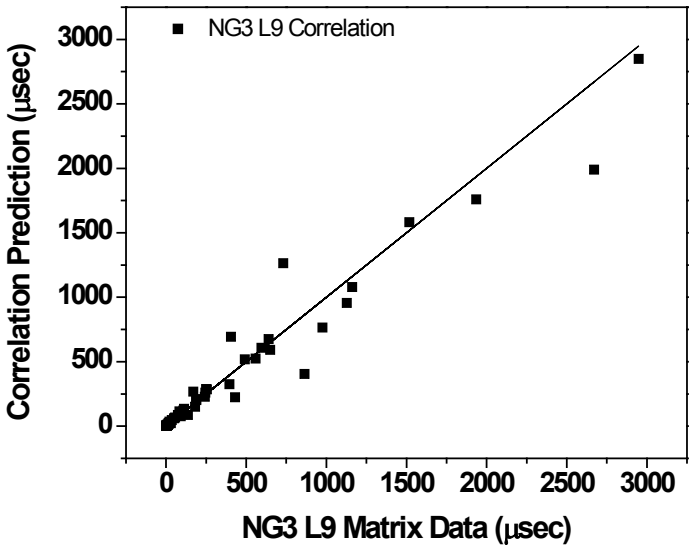

Figure 45 Comparison of the data used in the NG3 L9 matrix to the NG3 L9 matrix correlation. The predicted data are plotted as a function of the real data values with a 1 to 1 line.

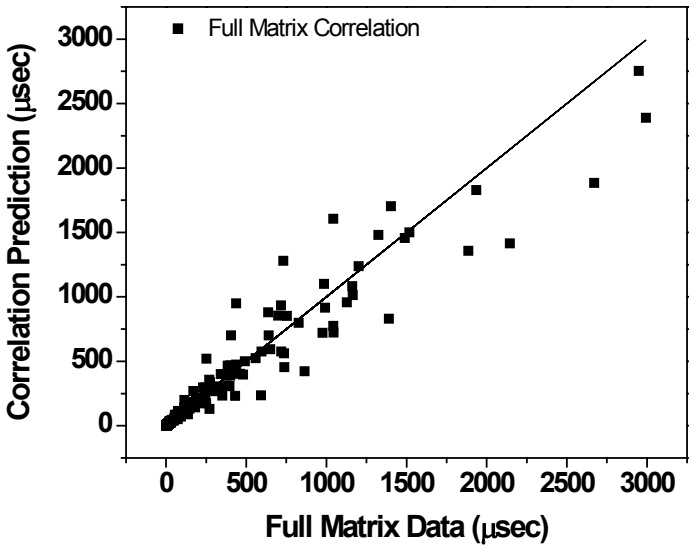

Figure 46 Comparison of the data used in the full matrix to the NG3 full matrix correlation. The predicted data are plotted as a function of the real data values with a 1 to 1 line.

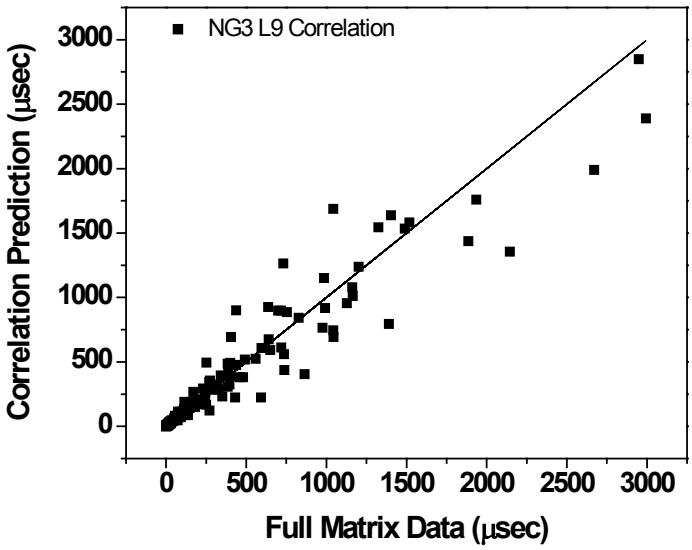

Figure 47 Comparison of the data used in the full matrix to the NG3 L9 matrix correlation. The predicted data are plotted as a function of the real data values with a 1 to 1 line.

Finally, a factor sensitivity analysis was performed for the NG3 L9 matrix. Since the correlations from the L9 matrix and the full matrix were found to be almost identical, only the 9 combinations from the L9 matrix were used for the factor sensitivity. Listed in Table 25 are correlations found for each individual combination of the NG3 L9 matrix. These correlations were used to predict the ignition delay times of each combination at a few different temperatures.

Table 25 Correlations for individual combinations of the NG3 L9 matrix.

Combo	A	E (kcal/mol)
1	5.12×10^{-5}	40.9
2	1.17×10^{-5}	41.7
3	4.87×10^{-6}	42.1
4	6.44×10^{-6}	43.5
5	1.17×10^{-4}	39.8
6	2.53×10^{-5}	36.8
7	3.10×10^{-5}	41.9
8	1.22×10^{-6}	46.4
9	4.20×10^{-4}	32.5

A factor sensitivity was performed on the L9 matrix, as described previously. Ignition delay times were found at the same four temperatures (1100 K, 1150 K, 1200 K, and 1250 K), and the factor sensitivities for each factor were normalized at each temperature. As seen Figure 48, the results are slightly different for NG3 than for the previous combinations. Hydrogen and pressure are almost equally important. For the two lower temperatures, hydrogen is most important, while at the two higher temperatures, pressure

is actually the most important. This is likely different for NG3 because of the high level of higher-order hydrocarbons in NG3. Since there are more higher-order hydrocarbons in NG3 than in CH_4 and NG2, the reactivity of the base natural gas is closer to that of pure hydrogen and, therefore, the addition of hydrogen does not change the reactivity as much. The effect of equivalence ratio is more important than what was seen in methane and NG2 and is almost equal to the effect of hydrogen at the highest temperature.

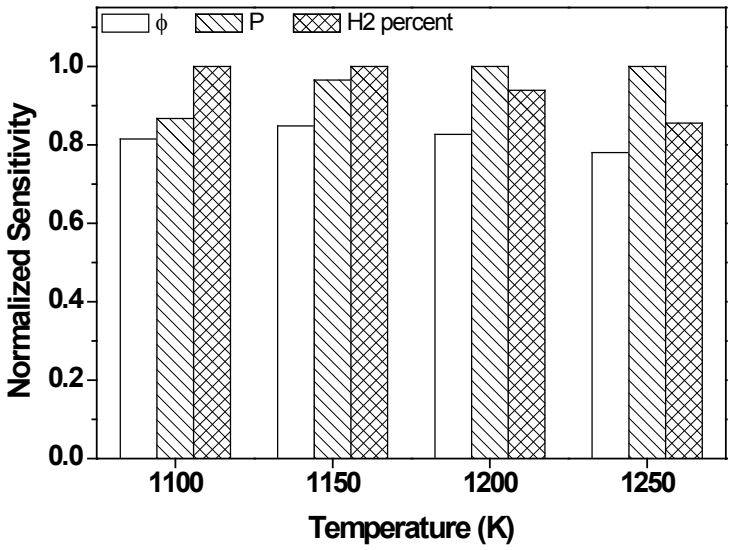

Figure 48 Factor sensitivity of the NG3 L9 matrix at four temperatures (1100 K, 1150 K, 1200 K, and 1250 K) for the three factors of the matrix (H_2 content of the fuel, equivalence ratio, and pressure).

CHAPTER VI

CONCLUSION

Variations in fuel composition drive the need for fuel flexibility in gas turbine combustors. Recently, interest has grown in using natural gases with high levels of hydrogen in current gas turbines. For reheat gas turbines, the ignition delay times of different fuels are of interest for two reasons: first, the ignition delay time must be longer than the residence time of the fuel in the mixer before the primary burner to prevent early ignition; and second, the ignition delay time must allow for stabilization of the flame in the secondary burner. Although there have been multiple studies on hydrogen ignition delay times and on ignition delay times of the various hydrocarbons of which most natural gases are composed, there have been few experimental studies performed on the ignition delay times of natural gases with high levels of hydrogen.

The study described herein looked at the impact of four different factors on ignition delay time: higher-order hydrocarbon content of a natural gas, hydrogen content of a fuel mixture, equivalence ratio, and pressure. An L9 matrix was developed to study all four factors in an efficient manner, and each factor was given three levels: higher-order hydrocarbon content was 0, 18.75, or 37.5%; hydrogen content of the total fuel mixture was 30, 60, or 80%; equivalence ratio was 0.3, 0.5, or 1; and experiments were performed at pressures of 1, 10, or 30 atm. Shock-tube experiments were performed for nine combinations of these factors with mixtures that were diluted in 90%, and experimental temperatures ranged from 1092 K to 1722 K. The Galway chemical

kinetics model was used to predict each experiment and, generally, the Galway model showed good agreement with the data from the experiments. Correlations were developed from the experimental data for each individual combination, for each natural gas mixture set (i.e. one for combinations containing methane, one for combinations containing NG2, and one for combinations containing NG3), and for the entire L9 matrix data set. The correlations developed using more than one combination generally predicted the data well but are not recommended for use outside of the experimental conditions used herein.

Using the correlations for each individual combination, a factor sensitivity analysis was performed for ignition delay times at four temperatures: 1100 K, 1150 K, 1200 K, and 1250 K. It was found that hydrogen played the most significant role and pressure played an important role that was only slightly smaller than the role of hydrogen, especially as temperature increased. The effect of equivalence ratio on ignition delay times was moderate and always less than the effects of pressure or hydrogen content. Higher-order hydrocarbon content was seen to have the smallest effect on ignition delay time but was not negligible.

Further calculations were performed using the Galway chemical kinetics mechanism for all possible combinations that could be made from the three different levels of each factor. Using the calculations, correlations were developed separately for combinations containing methane, NG2, and NG3. Additionally, correlations were found from L9

matrices that were developed for each baseline natural gas. A comparison between the correlations from the full matrix calculations and from the calculations for the L9 matrix for each natural gas showed the predictions were similar for both correlations. Additionally, data points that were poorly predicted by one correlation were also poorly predicted by the other. Although it was determined that these linear correlations could not completely capture the ignition delay time changes due to the complicated impact of hydrogen addition, the comparison proved that a reduced L9 matrix could indeed capture the same trends and produce a similar correlation to that provided by the full matrix.

It is recommended that further experiments be performed to develop correlations for each baseline natural gas that can be used outside of the experimental conditions herein. These additional experiments would improve the predicting capability of the correlations for each natural gas set. Moreover, experiments for each of the L9 matrices presented for the individual natural gases would provide three comprehensive correlations that could be used for different pressures, levels of hydrogen addition, and equivalence ratios. Furthermore, to develop correlations that properly predict the effect of hydrogen addition, it is recommended that other correlation methods be explored.

REFERENCES

Aul, C.J. (2009) An Experimental Study into the Ignition of Methane and Ethane Blends in a New Shock-Tube Facility. A Thesis, Texas A&M University.

Bourque, G., Healy, D., Curran, H., Zinner, C., Kalitan, D., de Vries, J., Aul, C., and Petersen, E. (2010) Ignition and Flame Speed Kinetics of Two Natural Gas Blends with High Levels of Heavier Hydrocarbons. *J. Eng. Gas Turbines Power*, **132**, 21504-21504.

Brower, M., Petersen, E., Metcalfe, W., Curran, H., Furi, M., Bourque, G., Aluri, N., and Guethe, F. (2012) Ignition Delay Time and Laminar Flame Speed Calculations for Natural Gas/Hydrogen Blends at Elevated Pressures. *ASME Paper GT2012-69310*, *ASME Turbo Expo,* June 11-15, 2012, Copenhagen, Denmark.

Cheng, R.K., and Oppenheim, A.K. (1984) Autoignition in Methane-Hydrogen Mixtures. *Combust. Flame*, **58**, 125-139.

Crossley, R.W., Dorko, E.A., Scheller, K., and Burcat, A. (1972) The Effect of Higher Alkanes on the Ignition of Methane-Oxygen-Argon Mixtures in Shock Waves. *Combust. Flame*, **19**, 373-378.

Davis, S.G., Law, C.K., and Wang, H. (1999) Propene Pyrolysis and Oxidation Kinetics in a Flow Reactor and Laminar Flames. *Combust. Flame*, **199**, 375-399.

de Vries, J., and Petersen, E.L. (2007) Autoignition of methane-based fuel blends under gas turbine conditions. *Proc. Combust. Instit.*, **31**, 3163-3171.

Donato, N.S., and Petersen, E.L. (2008) Simplified Correlation Models for CO/H_2 Chemical Reaction Times. *Int. J. Hydrogen Energy*, **33**, 7565-7579.

Fleck, J., Griebel, P., Steinberg, A.M., Stoehr, M., Aigner, M., and Ciani, A. (2012) Autoignition Limits of Hydrogen at Relevant Reheat Combustor Operating Conditions. *J. Eng. Gas Turbines Power*, **134**, 41502-41502.

Fotache, C.G., Kreutz, T.G., and Law, C.K. (1997) Ignition of Hydrogen-Enriched Methane by Heated Air. *Combust. Flame*, **110**, 429-440.

Güthe, F., Hellat, J., and Flohr, P. (2009) The Reheat Concept: The Proven Pathway to Ultralow Emissions and High Efficiency and Flexibility. *J. Eng. Gas Turbines Power*, **131**, 21503 – 21503.

Hall, J.M., and Petersen, E.L. (2006) An Optimized Kinetics Model for OH Chemiluminescence at High Temperatures and Atmospheric Pressures. *Int. J. Chem. Kinet.,***38**, 714-724.

Healy, D., Kopp, M.M., Polley, N.L., Petersen, E.L., Bourque, G., Curran, H.J., (2010-a) Methane/*n*-Butane Ignition Delay Measurements at High Pressure and Detailed Chemical Kinetic Simulations. *Energy Fuels*, **24**, 1617-1627.

Healy, D., Kalitan, D.M., Aul, C.J., Petersen, E.L., Bourque, G., and Curran, H.J. (2010-b) Oxidation of C1-C5 Alkane Quinternary Natural Gas Mixtures at High Pressures. *Energy Fuels*, **24**, 1521-1528.

Herzler, J. and Naumann, C. (2009) Shock-tube Study of the Ignition of Methane/Ethane/Hydrogen Mixtures with Hydrogen Contents from 0% to 100% at Different Pressures. *Proc. Combust. Instit.,* **32**, 213-220.

Higgin, R.M.R., Williams, A. (1969) A Shock-Tube Investigation of the Ignition of Lean Methane and *n*-Butane Mixtures with Oxygen. *Proc. Combust. Instit.*, **12**, 579-590.

Holton, M. M., Gokularkrishnan, P., Klassen, M.S., Roby, R.J., and Jackson, G.S. (2010) Autoignition Delay Time Measurements of Methane, Ethane, and Propane Pure Fuels and Methane-Based Fuel Blends. *J. Eng. Gas Turbines Power*, **132**, 91502 – 91502.

Huang, J., Bushe, W.K., Hill, P.G., and Munshi, S.R. (2006) Experimental and Kinetic Study of Shock Initiated Ignition in Homogeneous Methane-Hydrogen-Air Mixtures at Engine-Relevant Conditions. *Int. J. Chem. Kinet.*, **38**, 221-233.

Huang, J., Hill, P.G., Bushe, W.K., and Munshi, S.R. (2003) Shock-Tube Study of Methane Ignition under Engine-Relevant Conditions: Experiments and Modeling. *Combust. Flame,* **136**, 25-42.

Reaction Design, Inc. (2011) *CHEMKIN 10112*, San Diego.

Laskin, A., Wang, H., and Law, C.K. (2000) Detailed Kinetic Model of 1,3-Butadiene Oxidation at High Temperatures. *Int. J. Chem. Kinet.*, **32**, 589-614.

Law, C.K., (2006) *Combustion Physics*, 1st ed. Cambridge University Press, New York, 89-93.

Lieuwen, T., McDonell, V., Petersen, E., and Santavicca, D. (2008) Fuel Flexibility Influences on Premixed Combustor Blowout, Flashback, Autoignition, and Stability. *J. Eng. Gas Turbines Power,* **130**, 11506-11506.

Lifshitz, A., Scheller, K., Burcat, A., and Skinner, G.B. (1971) Shock-Tube Investigation of Ignition in Methane-Oxygen-Argon Mixtures. *Combust. Flame*, **16**, 311-321.

Metcalfe, W.K., Burke, S.M., Aul, C.J., Petersen, E.L., and Curran, H.J. (2011) A Detailed Chemical Kinetic Modelling and Experimental Study of C_1 – C_2 Hydrocarbons. *Fifth Europ. Combust. Meet.,* June 28 – July 1, 2011, Cardiff, Wales.

Ó Conaire, M., Curran, H.J., Simmie, J.M., Pitz, W.J., and Westbrook, C.K. (2004) A Comprehensive Modeling Study of Hydrogen Oxidation. *Int. J. Chem. Kinet.*, **36**, 603-622.

Petersen, E.L. (2009) Interpreting Endwall and Sidewall Measurements in Shock-Tube Ignition Studies. *Combust. Sci. Tech.*, **181**, 1123-1144.

Petersen, E.L., Hall, J.M., Smith, S.D., de Vries, J., Amadio, A.R., and Crofton, M.W. (2007-a) Ignition of Lean Methane-Based Fuel Blends at Gas Turbine Pressures. *J. Eng. Gas Turbine Power*, **129**, 937-944.

Petersen, E.L., Kalitan, D.M., Simmons, S., Bourque, G., Curran, H.J., Simmie, J.M. (2007-b) Methane/Propane Oxidation at High Pressures: Experimental and Detailed Chemical Kinetic Modeling. *Proc. Combust. Instit.,* **31**, 447-454.

Petersen, E.L., Rickard, M.J.A., Crofton, M.W., Abbey, E.D., Traum, M.J., and Kalitan D.M. (2005) A Facility for Gas- and Condensed-Phase Measurements Behind Shock Waves. *Meas. Sci. Technol*., **16**, 1716.

Ross, P.J. (1988) *Taguchi Techniques for Quality Engineering*. McGraw-Hill, New York, 101-114.

Slack, M.W. (1977) Rate Coefficient for $H + O_2 + M = HO_2 + M$ Evaluated from Shock Tube Measurements of Induction Times. *Combust. Flame*, **28**, 241-249.

Spadaccini, L. J., and Colket III, M. B. (1994) Ignition delay characteristics of methane fuels. *Prog. Energy Combust. Sci.*, **20**, 431-460.

Turns, S.R. (2000) *An Introduction to Combustion: Concepts and Applications*, 2nd ed., McGraw Hill, Boston, 253-283.

Zhang, Y., Zuohua, H., Wei, L. Zhang, J., and Law, C.K. (2012) Experimental and Modeling Study on Ignition Delays of Lean Mixtures of Methane, Hydrogen, Oxygen, and Argon at Elevated Pressures. *Combust. Flame*, **159**, 918-931.

APPENDIX

Table 26 Experimental data and conditions for combination 1.

CH_4 (%)	H_2 (%)	O_2 (%)	Ar (%)	H_2 (% fuel)	ϕ	P (atm)	T (K)	τ_{ign} (μsec)
1.14	0.487	8.38	90	30	0.3	1.67	1283	1764.1
1.14	0.487	8.38	90	30	0.3	1.62	1311	1108.7
1.14	0.487	8.38	90	30	0.3	1.62	1354	865.3
1.14	0.487	8.38	90	30	0.3	1.59	1397	574.1
1.14	0.487	8.38	90	30	0.3	1.60	1454	460.7
1.14	0.487	8.38	90	30	0.3	1.56	1529	289.2
1.14	0.487	8.38	90	30	0.3	1.55	1555	195.8
1.14	0.487	8.38	90	30	0.3	1.54	1600	169.9
1.14	0.487	8.38	90	30	0.3	1.51	1645	132.7
1.14	0.487	8.38	90	30	0.3	1.55	1722	98.7

Table 27 Experimental data and conditions for combination 2.

CH_4 (%)	H_2 (%)	O_2 (%)	Ar (%)	H_2 (% fuel)	ϕ	P (atm)	T (K)	τ_{ign} (μsec)
1.25	1.88	6.88	90	60	0.5	10.32	1116	1902.9
1.25	1.88	6.88	90	60	0.5	10.17	1141	1144.1
1.25	1.88	6.88	90	60	0.5	10.10	1153	972.6
1.25	1.88	6.88	90	60	0.5	9.86	1168	651.8
1.25	1.88	6.88	90	60	0.5	9.81	1186	504.5
1.25	1.88	6.88	90	60	0.5	9.77	1214	411.9
1.25	1.88	6.88	90	60	0.5	10.49	1234	325.6
1.25	1.88	6.88	90	60	0.5	10.01	1250	255.4
1.25	1.88	6.88	90	60	0.5	10.01	1286	165.0
1.25	1.88	6.88	90	60	0.5	10.00	1317	118.7

Table 28 Experimental data and conditions for combination 3.

CH_4 (%)	H_2 (%)	O_2 (%)	Ar (%)	H_2 (% fuel)	ϕ	P (atm)	T (K)	τ_{ign} (μsec)
1.11	4.44	4.45	90	80	1	32.54	1110	1296.2
1.11	4.44	4.45	90	80	1	32.10	1116	1195.5
1.11	4.44	4.45	90	80	1	31.25	1117	1226.8
1.11	4.44	4.45	90	80	1	31.38	1144	748.1
1.11	4.44	4.45	90	80	1	30.67	1148	642.0
1.11	4.44	4.45	90	80	1	30.07	1163	543.8
1.11	4.44	4.45	90	80	1	30.45	1189	382.5
1.11	4.44	4.45	90	80	1	30.02	1206	259.0
1.11	4.44	4.45	90	80	1	29.52	1220	230.0

Table 29 Experimental data and conditions for combination 4.

NG2 (%)	H_2 (%)	O_2 (%)	Ar (%)	H_2 (% fuel)	ϕ	P (atm)	T (K)	τ_{ign} (μsec)
1.46	0.63	7.91	90	30	0.5	33.2	1152	1525.7
1.46	0.63	7.91	90	30	0.5	33.6	1168	1223.1
1.46	0.63	7.91	90	30	0.5	33.7	1180	1017.3
1.46	0.63	7.91	90	30	0.5	32.7	1191	899.1
1.46	0.63	7.91	90	30	0.5	32.9	1213	683.0
1.46	0.63	7.91	90	30	0.5	32.3	1222	590.6
1.46	0.63	7.91	90	30	0.5	33.6	1225	612.7
1.46	0.63	7.91	90	30	0.5	32.3	1246	436.3
1.46	0.63	7.91	90	30	0.5	31.8	1257	376.8
1.46	0.63	7.91	90	30	0.5	31.6	1299	250.3

Table 30 Experimental data and conditions for combination 5.

NG2 (%)	H_2 (%)	O_2 (%)	Ar (%)	H_2 (% fuel)	ϕ	P (atm)	T (K)	τ_{ign} (μsec)
1.74	2.61	5.64	90	60	1	1.72	1203	1779.4
1.74	2.61	5.64	90	60	1	1.71	1220	1546.8
1.74	2.61	5.64	90	60	1	1.72	1241	1133.6
1.74	2.61	5.64	90	60	1	1.64	1266	817.7
1.74	2.61	5.64	90	60	1	1.66	1295	620.5
1.74	2.61	5.64	90	60	1	1.66	1309	534.9
1.74	2.61	5.64	90	60	1	1.71	1346	329.9
1.74	2.61	5.64	90	60	1	1.66	1349	321.9
1.74	2.61	5.64	90	60	1	1.68	1382	279.6
1.74	2.61	5.64	90	60	1	1.64	1387	261.7
1.74	2.61	5.64	90	60	1	1.61	1404	192.9
1.74	2.61	5.64	90	60	1	1.64	1443	169.6

Table 31 Experimental data and conditions for combination 6.

NG2 (%)	H_2 (%)	O_2 (%)	Ar (%)	H_2 (% fuel)	ϕ	P (atm)	T (K)	τ_{ign} (μsec)
0.501	2.00	7.49	90	80	0.3	10.24	1092	1593.4
0.501	2.00	7.49	90	80	0.3	9.87	1101	1423.3
0.501	2.00	7.49	90	80	0.3	10.34	1118	820.2
0.501	2.00	7.49	90	80	0.3	10.35	1129	615.9
0.501	2.00	7.49	90	80	0.3	10.23	1131	557.9
0.501	2.00	7.49	90	80	0.3	10.02	1145	464.4
0.501	2.00	7.49	90	80	0.3	10.24	1147	419.6
0.501	2.00	7.49	90	80	0.3	10.24	1166	364.8
0.501	2.00	7.49	90	80	0.3	10.07	1168	302.5
0.501	2.00	7.49	90	80	0.3	10.48	1187	295.2
0.501	2.00	7.49	90	80	0.3	10.33	1196	188.6

Table 32 Experimental data and conditions for combination 7.

NG3 (%)	H_2 (%)	O_2 (%)	Ar (%)	H_2 (% fuel)	ϕ	P (atm)	T (K)	τ_{ign} (μsec)
2.17	0.928	6.91	90	30	1	9.76	1192	1584.4
2.17	0.928	6.91	90	30	1	9.63	1199	1404.1
2.17	0.928	6.91	90	30	1	9.60	1214	1274.0
2.17	0.928	6.91	90	30	1	9.37	1228	1039.7
2.17	0.928	6.91	90	30	1	9.97	1258	623.3
2.17	0.928	6.91	90	30	1	9.75	1261	598.7
2.17	0.928	6.91	90	30	1	10.14	1302	401.7
2.17	0.928	6.91	90	30	1	9.95	1312	370.6
2.17	0.928	6.91	90	30	1	9.35	1335	303.5
2.17	0.928	6.91	90	30	1	10.02	1349	257.3
2.17	0.928	6.91	90	30	1	9.97	1374	204.6
2.17	0.928	6.91	90	30	1	9.87	1381	186.4

Table 33 Experimental data and conditions for combination 8.

NG3 (%)	H_2 (%)	O_2 (%)	Ar (%)	H_2 (% fuel)	ϕ	P (atm)	T (K)	τ_{ign} (μsec)
0.670	1.01	8.32	90	60	0.3	33.2	1134	1377.1
0.670	1.01	8.32	90	60	0.3	32.8	1158	949.5
0.670	1.01	8.32	90	60	0.3	33.6	1161	853.1
0.670	1.01	8.32	90	60	0.3	32.1	1167	726.6
0.670	1.01	8.32	90	60	0.3	32.7	1190	531.7
0.670	1.01	8.32	90	60	0.3	32.9	1198	455.1
0.670	1.01	8.32	90	60	0.3	32.3	1206	416.4
0.670	1.01	8.32	90	60	0.3	32.2	1225	303.9
0.670	1.01	8.32	90	60	0.3	32.3	1247	231.8
0.670	1.01	8.32	90	60	0.3	31.9	1253	213.5

Table 34 Experimental data and conditions for combination 9.

NG3 (%)	H_2 (%)	O_2 (%)	Ar (%)	H_2 (% fuel)	ϕ	P (atm)	T (K)	τ_{ign} (μsec)
0.669	2.68	6.66	90	80	0.5	1.87	1112	1330.5
0.669	2.68	6.66	90	80	0.5	1.77	1121	1189.2
0.669	2.68	6.66	90	80	0.5	1.81	1151	793.4
0.669	2.68	6.66	90	80	0.5	1.77	1152	713.2
0.669	2.68	6.66	90	80	0.5	1.79	1177	580.8
0.669	2.68	6.66	90	80	0.5	1.76	1183	501.8
0.669	2.68	6.66	90	80	0.5	1.70	1219	336.2
0.669	2.68	6.66	90	80	0.5	1.66	1233	258.7
0.669	2.68	6.66	90	80	0.5	1.67	1258	207.5
0.669	2.68	6.66	90	80	0.5	1.68	1280	174.5

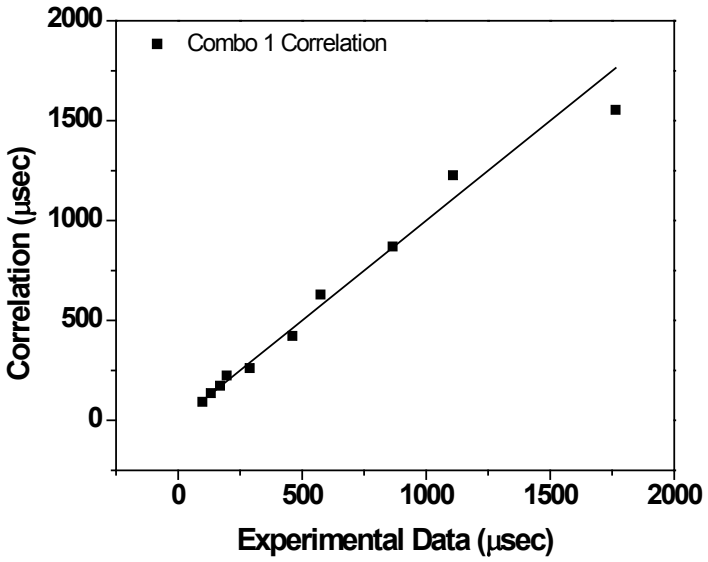

Figure 49 Comparison of combination 1 data to the combination 1 correlation. The predicted data are plotted as a function of the real data values with a 1 to 1 line.

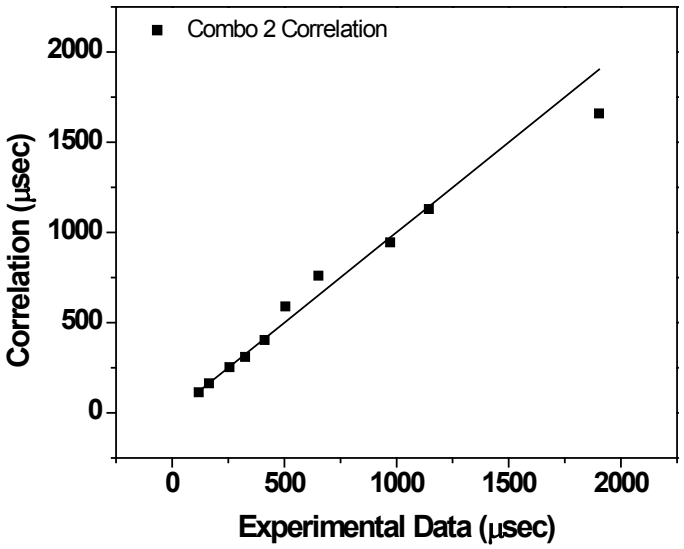

Figure 50 Comparison of combination 2 data to the combination 2 correlation. The predicted data are plotted as a function of the real data values with a 1 to 1 line.

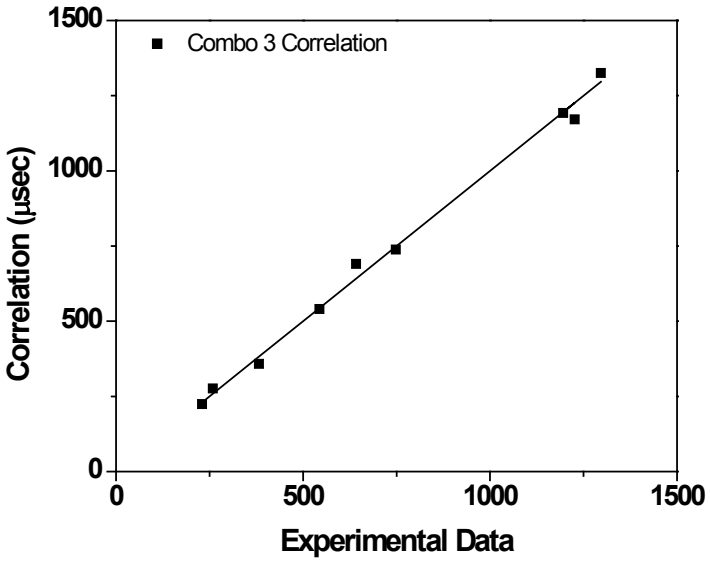

Figure 51 Comparison of combination 3 data to the combination 3 correlation. The predicted data are plotted as a function of the real data values with a 1 to 1 line.

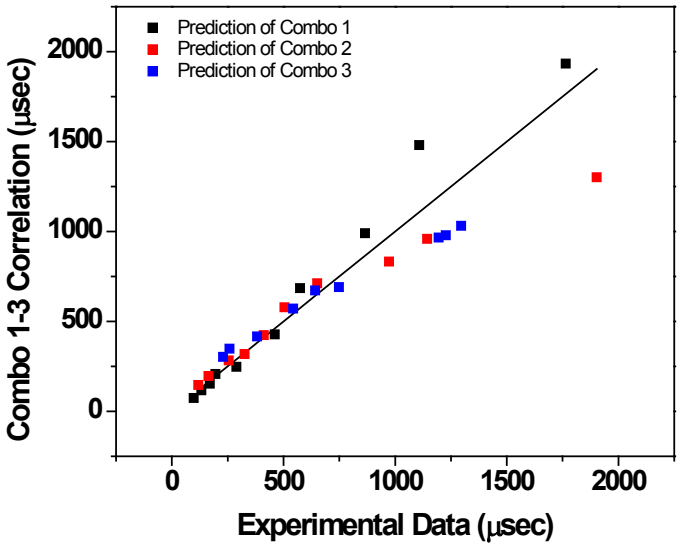

Figure 52 Comparison of the data from combinations 1, 2 and 3 to the correlation for combinations 1, 2 and 3. The predicted data are plotted as a function of the real data values with a 1 to 1 line.

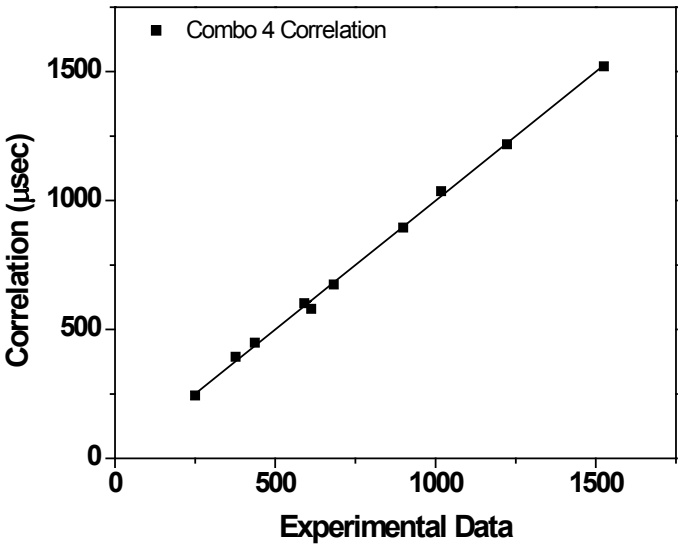

Figure 53 Comparison of combination 4 data to the combination 4 correlation. The predicted data are plotted as a function of the real data values with a 1 to 1 line.

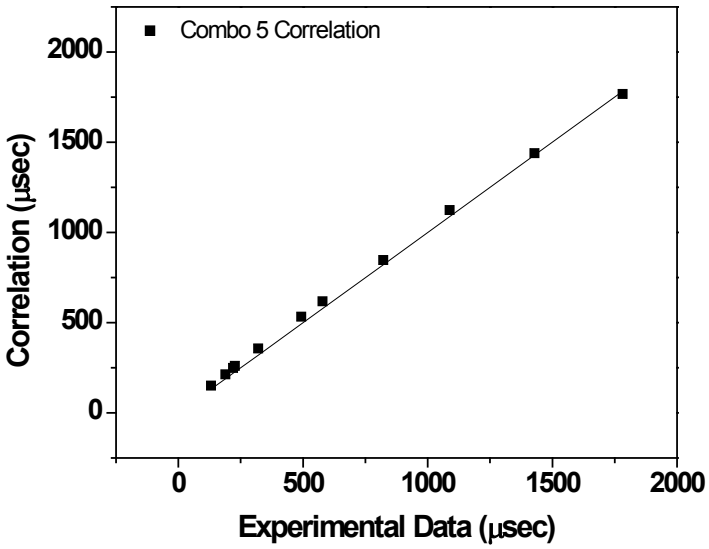

Figure 54 Comparison of combination 5 data to the combination 5 correlation. The predicted data are plotted as a function of the real data values with a 1 to 1 line.

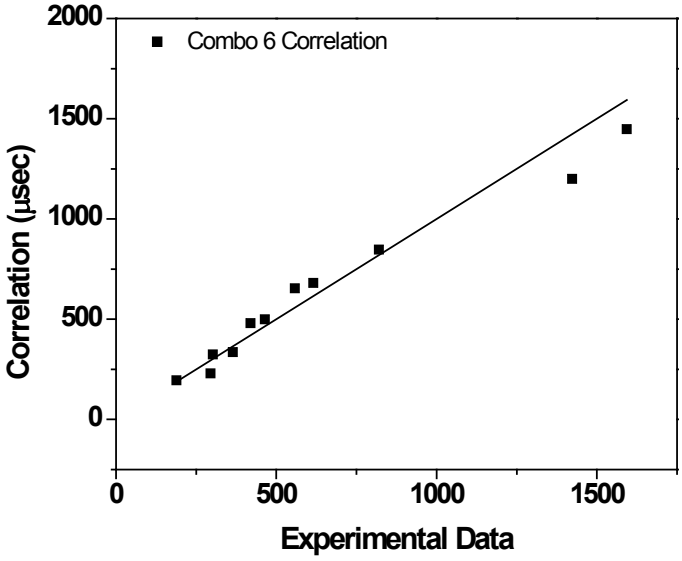

Figure 55 Comparison of combination 6 data to the combination 6 correlation. The predicted data are plotted as a function of the real data values with a 1 to 1 line.

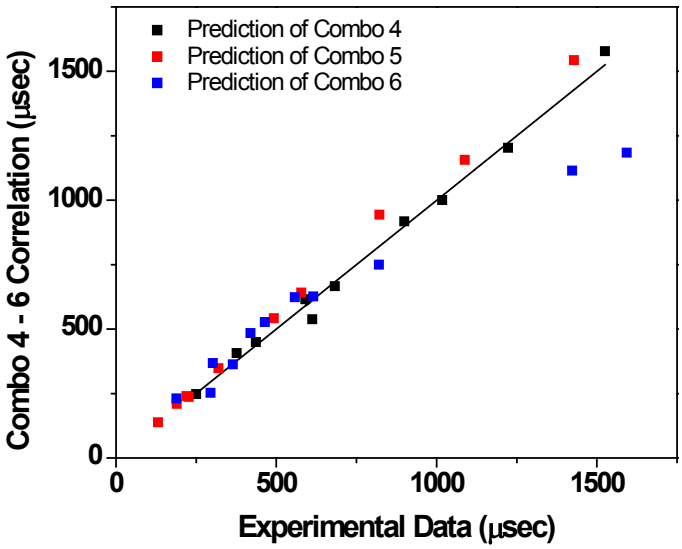

Figure 56 Comparison of the data from combinations 4, 5, and 6 to the correlation for combinations 4, 5, and 6. The predicted data are plotted as a function of the real data values with a 1 to 1 line.

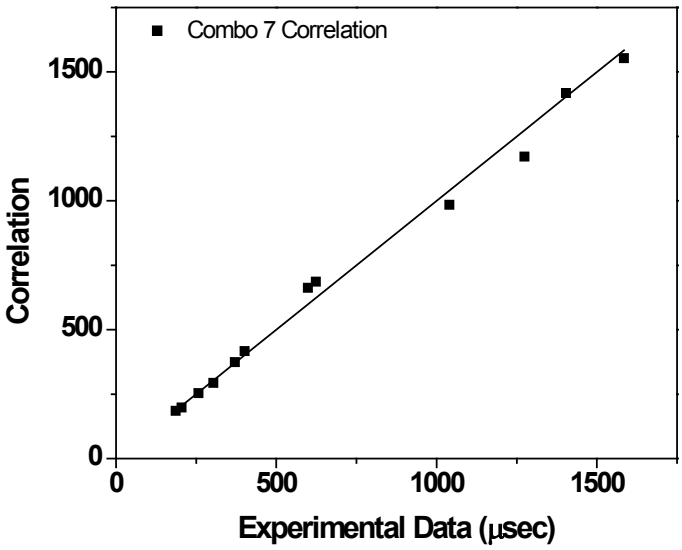

Figure 57 Comparison of combination 7 data to the combination 7 correlation. The predicted data are plotted as a function of the real data values with a 1 to 1 line.

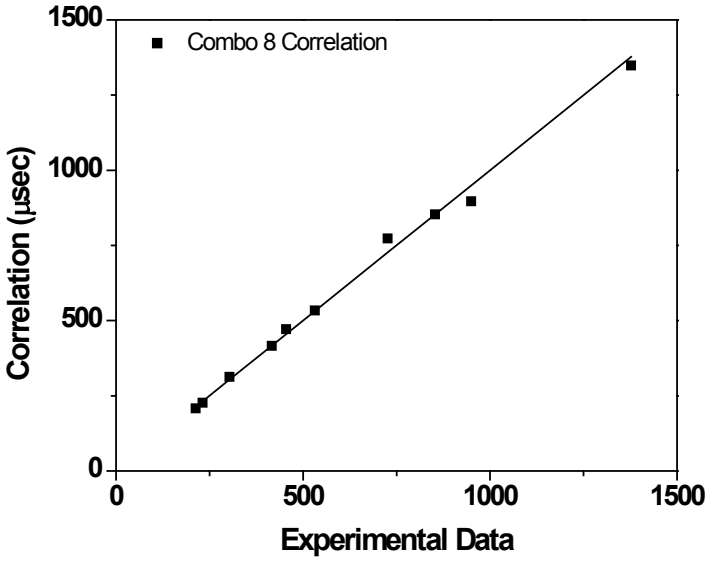

Figure 58 Comparison of combination 8 data to the combination 8 correlation. The predicted data are plotted as a function of the real data values with a 1 to 1 line.

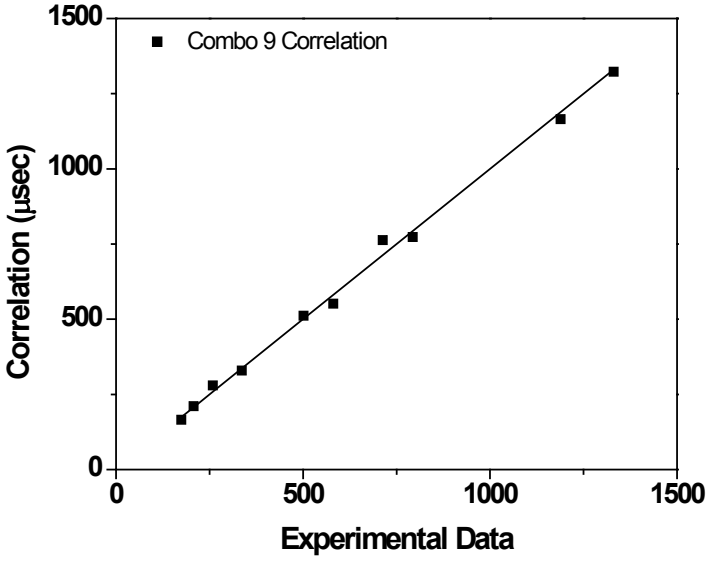

Figure 59 Comparison of combination 9 data to the combination 9 correlation. The predicted data are plotted as a function of the real data values with a 1 to 1 line.

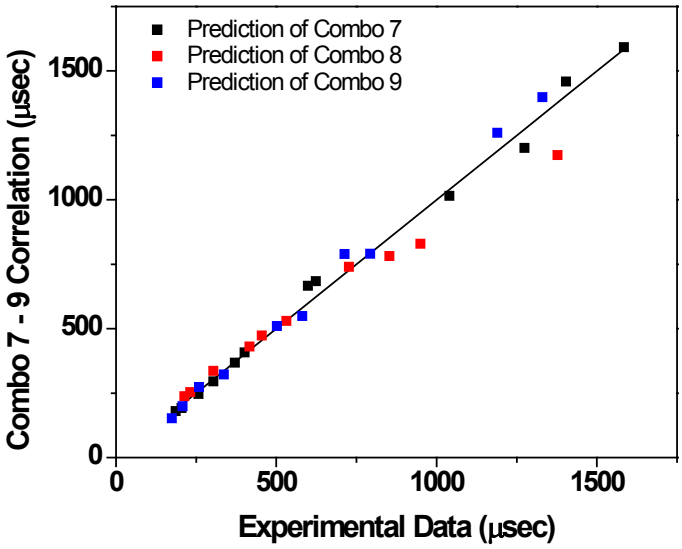

Figure 60 Comparison of the data from combinations 7, 8, and 9 to the correlation for combinations 7, 8, and 9. The predicted data are plotted as a function of the real data values with a 1 to 1 line.